Inexact primal–dual active set method for solving elastodynamic frictional contact problems

Stéphane Abide, Mikaël Barboteu, Soufiane Cherkaoui, David Danan, Serge Dumont

Inexact primal–dual active set method for solving elastodynamic frictional contact problems

Stéphane Abide [a], Mikaël Barboteu [a,*], Soufiane Cherkaoui [a], David Danan [b], Serge Dumont [c]

[a] Laboratoire de Mathématiques et Physique, Université de Perpignan Via Domitia, 52 Avenue Paul Alduy, 66860 Perpignan, France
[b] Institut de Recherche Technologique SystemX, Centre d'intégration Nano-INNOV, 8, Avenue de la Vauve, 91127 Palaiseau CEDEX, France
[c] Institut Montpelliérain Alexander Grothendieck, Université de Nîmes, Site des Carmes, Place Gabriel Péri, 30000 Nîmes, France

ARTICLE INFO

Article history:
Received 31 January 2020
Received in revised form 26 September 2020
Accepted 28 November 2020
Available online 17 December 2020

Keywords:
Unilateral constraint
Friction law
Hyper-elasticity
Dynamics
Semismooth Newton method
Primal–Dual Active Set

ABSTRACT

In this paper, several active set methods based on classical problems arising in Contact Mechanics are analyzed, namely unilateral/bilateral contact associated with Tresca's/Coulomb's law of friction in small and large deformation. The purpose of this work is to extend an Inexact Primal–Dual Active Set (IPDAS) method already used in Hueber et al. (2008) to the formalism of dynamics and hyper-elasticity. This method permits to solve the unilateral problem with Coulomb's law of friction by taking into account an alternative for the latter based on the approximation of the Coulomb's law by a succession of states of Tresca friction in which the friction threshold is fixed at each fixed point iteration. The mechanical formulation in the hyper-elasticity framework is first presented, next, we establish weak formulations of the different cases of frictional contact problems and we give the finite element approximation of the problems. Then, we detail the numerical treatment within the framework of the primal–dual active set strategy for different frictional contact conditions. We finally provide some numerical experiments to bring into light the efficiency of the IPDAS method and to carry out a comparison with the augmented Lagrangian method by considering representative contact problems in both small and large deformation cases.

1. Introduction

Frictional contact boundary condition remains an important basic concept to mathematical and numerical analysis of contact dynamics. In literature, many references come up with usual contact conditions approaches (cf [1–12]), since unilateral constraints and Coulomb friction generally lead to a non-linear and non-smooth mathematical problem. To handle the non-linearities due to the frictional contact conditions, several methods have been successfully tested, namely, the penalty method (cf [13,14]) which consist in approximating the original conditions by simpler ones, the quasi-augmented lagrangian [1], the bi-potential method (cf [15,16]), the conjugate gradient method (cf [9,12]), Uzawa method (cf [10,17]) and Nitsche finite element method (cf [5,18,19] and references therein). Alart and Curnier [1] proposed a quasi-augmented Lagrangian formulation combined with a Generalized Newton method to solve these continuous but

* Corresponding author.
E-mail addresses: stephane.abide@univ-perp.fr (S. Abide), barboteu@univ-perp.fr (M. Barboteu), soufiane.cherkaoui@univ-perp.fr (S. Cherkaoui), daviddanan9021@gmail.com (D. Danan), serge.dumont@unimes.fr (S. Dumont).

non-differentiable equations. Similarly, De Saxcé and Feng proposed in [15] so-called bi-potential energy to take into account the frictional contact. The bi-potential, which is not globally convex, is based on the theory of Implicit Standard Material and it is minimized generally using a gradient method. The Nitsche finite element method consists of writing the contact and frictional conditions directly in the variational formulation, leading to a straightforward finite element method and a non-linear discretized problem. Let us notice that, in a numerical treatment, all these methods can be extended to an integral formulation, except the bi-potential method that have to be considered at each node of the mesh of a finite element method.

Lately, Primal–Dual Active Set strategies (PDAS) arise as one of the most prominent methods for solving frictional contact problems (cf [20–22]). The main purpose of such methods is to separate the set of nodes that can be in contact into two subsets: the first subset $\mathcal{A}$ includes all nodes that are currently in contact (active) whereas the second subset $\mathcal{I}$ includes all the other nodes (inactive). In practical terms, PDAS do not require the use of the Lagrange multipliers. As a matter of fact, the boundary conditions on the nodes in the subsets $\mathcal{A}$ and $\mathcal{I}$ are classical and can be directly enforced. Some works have been dedicated to studying the efficiency of PDAS methods, as well as to solve non-linear multi-body contact problems in elastodynamics (cf [21,22]), or to solve linear elasticity problems with unilateral boundary conditions (cf [20,23]).

Hence, the novelty of this article is to propose an innovative, fast and efficient PDAS method to solve a problem of hyper-elastodynamics with unilateral contact and Coulomb friction. The idea of this paper is to present in detail the PDAS method for several frictional contact cases against a rigid foundation, namely the unilateral contact, the bilateral contact with Tresca's friction, and finally the unilateral contact with Coulomb's friction.

First, this work puts the light on the evolution of a hyper-elastodynamic body in bilateral contact with a rigid foundation. As the contact involves friction of Tresca type, a bilateral contact condition combined with a Tresca's law of friction is considered. Then, this paper extends this case to the unilateral case with Coulomb's law of friction, considering an alternative for the latter based on the approximation of the Coulomb's law by a succession of states of Tresca's friction, already used in [21] for elasto-statics. Second, Duvaut and Lions proposed in [24], a formulation based on the similarity between Tresca and Coulomb laws, applied numerically in [10] and [21] for Active Set. The Tresca's friction contact problem presents the advantage that it can be reduced to a problem of minimization under constraints. Here, more precisely, the idea is first to solve the problem with Tresca's friction threshold fixed, next to update this threshold according to the results obtained on the normal part of the contact efforts, and then to iterate this principle until sufficiently stable threshold values are obtained. The convergence of this fixed point method, has been proven in [25].

Moreover, the performance and the efficiency in terms of computational costs of PDAS strategies for non-linear and non-smooth problems, proven in [21,22,26], are very significant. Indeed, we provide in this work a comparison between PDAS methods and the quasi-augmented Lagrangian method, in terms of numerical accuracy, convergence rate and CPU time.

The discrete frictional contact conditions are realized by applying an active set strategy to the non-linear complementary function based on a Newton semi-smooth iterative scheme (cf [20,23]). For each case involving several frictional contact conditions, we present in detail the operators and the active and inactive sets which describe the non-linear equations arising from the discretized problems. Next, we describe the iterative active set algorithms for each type of frictional contact problems. In order to confront the PDAS to the quasi-augmented Lagrangian method for solving several frictional contact problem for hyper-elasticity, we mainly study and compare the properties of both methods in terms of numerical convergence with respect to several parameters such as the number of degrees of freedom, the number of iterations and the CPU time. Moreover, we also analyze the behavior of solutions considering various contact conditions.

The remainder of the article is organized as follows. In Section 2, we present both the mechanical problem and the variational formulation in the framework of hyper-elasticity. Section 3 is devoted to the discretization of the variational problem. In Section 4, we recall the frictionless unilateral contact law with a gap before applying an Active Set strategy for this law based on a Newton semi-smooth iterative scheme. Section 5 is dedicated to a bilateral contact condition combined with a Tresca's law of friction, whereas a unilateral contact with Coulomb's law of dry friction is considered in Section 6. Section 7 is divided into two parts. First, a full PDAS strategy for unilateral contact with Coulomb's friction law is considered. Next, an inexact PDAS with fixed point method related to the friction bound is introduced. Finally, Sections 8 and 9 are exclusively devoted to the numerical results, first in the static case then in the dynamic case.

2. Formulations of the dynamic contact problem

In this section the mechanical problem of hyper-elasticity and the associated variational formulation are presented.

2.1. Hyperelastodynamic contact model

Let us consider a hyper-elastic body which occupies a domain $\Omega \subset \mathbb{R}^d$ $(d = 1, 2, 3)$ of boundary Γ. The former is assumed Lipschitz continuous and consists in three disjoint measurable parts Γ_1, Γ_2 and Γ_3 such that $meas(\Gamma_1) > 0$. The notations $\boldsymbol{x} = (x_i)$ and $\boldsymbol{\nu} = (\nu_i)$ stand for a point in $\Omega \cup \Gamma$ and the outward unit normal at Γ, respectively. In what follows, the Einstein summation convention holds, and the indices i, j, k, l range between 1 and d. Let us denote by $\mathbb{M}^d$ the second

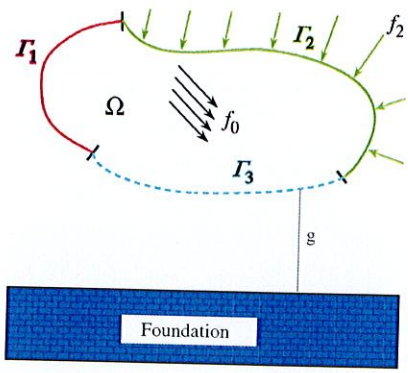

Fig. 1. Physical setting of a deformable body against a foundation.

order tensors space defined on $\mathbb{R}^d$ or, equivalently, the space of square matrices of order d. The usual inner product and norm on $\mathbb{R}^d$ and $\mathbb{M}^d$ reads:

$$\boldsymbol{u}\cdot\boldsymbol{v}=u_iv_i\,,\qquad \|\boldsymbol{v}\|=(\boldsymbol{v}\cdot\boldsymbol{v})^{\frac{1}{2}}\qquad \forall\,\boldsymbol{u},\,\boldsymbol{v}\in\mathbb{R}^d,$$
$$\boldsymbol{\Pi}:\boldsymbol{\gamma}=\Pi_{ij}\gamma_{ij}\,,\qquad \|\boldsymbol{\gamma}\|=(\boldsymbol{\gamma}:\boldsymbol{\gamma})^{\frac{1}{2}}\qquad \forall\,\boldsymbol{\Pi},\,\boldsymbol{\gamma}\in\mathbb{M}^d.$$

$\boldsymbol{u}$ denotes the displacement field and $\boldsymbol{\Pi}$ the first Piola–Kirchhoff stress tensor. The normal and the tangential components of $\boldsymbol{u}$ on Γ are given by $u_\nu=\boldsymbol{u}\cdot\boldsymbol{\nu}$ and $\boldsymbol{u}_\tau=\boldsymbol{u}-u_\nu\boldsymbol{\nu}$. Also, the normal and the tangential components Π_ν and $\boldsymbol{\Pi}_\tau$ are denoted by $\Pi_\nu=(\boldsymbol{\Pi}\boldsymbol{\nu})\cdot\boldsymbol{\nu}$ and $\boldsymbol{\Pi}_\tau=\boldsymbol{\Pi}\boldsymbol{\nu}-\Pi_\nu\boldsymbol{\nu}$. The divergence operator is defined by $\mathrm{Div}\,\boldsymbol{\Pi}=(\Pi_{ij,j})$. For the sake of clarity, a concise notation of the partial derivative is used : $u_{i,j}=\partial u_i/\partial x_j$.

We considered material described with a hyper-elastic constitutive law that is characterized by the first Piola–Kirchhoff tensor $\boldsymbol{\Pi}$. This former is derived from an internal hyper-elastic energy density $W:\Omega\times\mathbb{M}^d_+\to\mathbb{R}$, $\boldsymbol{\Pi}=\frac{\partial}{\partial\mathbf{F}}W(\boldsymbol{x},\mathbf{F})=\partial_{\mathbf{F}}W(\boldsymbol{x},\mathbf{F})$, for all $\boldsymbol{x}\in\Omega$ and $\mathbf{F}\in\mathbb{M}^d$. Here $\mathbf{F}$ is the deformation gradient defined by $\mathbf{F}=\mathbf{I}+\nabla\boldsymbol{u}$ and $\partial_{\mathbf{F}}$ represents the differential with respect to the variable $\mathbf{F}$ (cf [27,28]). In the following, the dynamic frictional contact of a hyper-elastic body with a perfectly rigid obstacle, the so-called foundation, is considered (see Fig. 1).

The hyper-elastic body displacement is driven by the body force of density $\boldsymbol{f}_0$ and the surface traction of density $\boldsymbol{f}_2$ that acts on Γ_2. The mechanical hyper-elastic problem is investigated on a time interval $[0,T]$ with $T>0$, and the time variable denoted by t. For the sake of conciseness, we do not refer to the dependence of the functions on $\boldsymbol{x}$ and t, and the derivatives with respect to the time reads $\dot{(.)}$. The displacement on the boundary Γ_1 is prescribed, and also on Γ_3 when the contact condition holds. The frictional contact conditions are formulated as the unilateral contact conditions combined to a Coulomb's law of dry friction. The unilateral contact relations on Γ_3 depend on the normal displacement u_ν and the normal contact pressure Π_ν as follows,

$$u_\nu\le g,\quad \Pi_\nu\le 0,\quad (u_\nu-g)\Pi_\nu=0, \tag{2.1}$$

where the gap g measures the distance between a point on Γ_3 and its projection onto the rigid obstacle. See [29] for further detail about large sliding frictional contact between deformable solids. The Coulomb's friction law depends on the tangential frictional stress $\boldsymbol{\Pi}_\tau$, the normal contact pressure Π_ν and the tangential contact velocity $\dot{\boldsymbol{u}}_\tau$ by these relations:

$$\|\boldsymbol{\Pi}_\tau\|\le\mu\,|\Pi_\nu|, \tag{2.2}$$
$$-\boldsymbol{\Pi}_\tau=\mu\,|\Pi_\nu|\,\frac{\dot{\boldsymbol{u}}_\tau}{\|\dot{\boldsymbol{u}}_\tau\|}\quad\text{if}\quad\dot{\boldsymbol{u}}_\tau\neq\mathbf{0}, \tag{2.3}$$

where μ denotes the coefficient of friction.

Using the previously introduced notations, the formulation of the dynamic contact problem in the framework of hyper-elasticity is:

Problem $\mathcal{P}$. *Find a displacement field* $\boldsymbol{u}:\Omega\times[0,T]\to\mathbb{R}^d$ *and a stress field* $\boldsymbol{\Pi}:\Omega\times[0,T]\to\mathbb{M}^d$ *such that*

$$\boldsymbol{\Pi}=\partial_{\mathbf{F}}W(\mathbf{F})\quad\text{in}\quad\Omega\times(0,T), \tag{2.4}$$
$$-\rho\ddot{\boldsymbol{u}}+\mathrm{Div}\,\boldsymbol{\Pi}+\boldsymbol{f}_0=\mathbf{0}\quad\text{in}\quad\Omega\times(0,T), \tag{2.5}$$
$$\boldsymbol{u}=\mathbf{0}\quad\text{on}\quad\Gamma_1\times(0,T), \tag{2.6}$$
$$\boldsymbol{\Pi}\boldsymbol{\nu}=\boldsymbol{f}_2\quad\text{on}\quad\Gamma_2\times(0,T), \tag{2.7}$$
$$u_\nu\le g,\quad\Pi_\nu\le 0,\quad(u_\nu-g)\Pi_\nu=0\quad\text{on}\quad\Gamma_3\times(0,T), \tag{2.8}$$
$$\begin{cases}\|\boldsymbol{\Pi}_\tau\|\le\mu\,|\Pi_\nu|,\\ -\boldsymbol{\Pi}_\tau=\mu\,|\Pi_\nu|\,\frac{\dot{\boldsymbol{u}}_\tau}{\|\dot{\boldsymbol{u}}_\tau\|}\quad\text{if}\quad\dot{\boldsymbol{u}}_\tau\neq\mathbf{0}.\end{cases}\quad\text{on}\quad\Gamma_3\times(0,T), \tag{2.9}$$

$$\boldsymbol{u}(0) = \boldsymbol{u}_0, \ \dot{\boldsymbol{u}}(0) = \boldsymbol{u}_1 \quad \text{in} \quad \Omega. \tag{2.10}$$

Compatibility conditions on the initial displacement are written as follows $\boldsymbol{\Pi}(\boldsymbol{x}, 0) = \partial_{\mathbf{F}} W(\boldsymbol{x}, \mathbf{I} + \nabla \boldsymbol{u}(\boldsymbol{x}, 0))$. The constitutive law of the material is described by Eq. (2.4). Eq. (2.5) represents the equation of motion in which ρ denotes the density of the material and is assumed to be constant, for the sake of simplicity. Conditions (2.6), (2.7) represent the displacement and traction boundary conditions, respectively. Finally, conditions (2.8) and (2.9) represent the frictional contact conditions previously described in this section. Note that the conditions (2.8) are equivalent to the following subdifferential inclusion (cf [30])

$$-\Pi_\nu \in \partial \Psi_{\mathbb{R}^-}(u_\nu - g) \quad \text{on } \Gamma_3 \times (0, T), \tag{2.11}$$

where ∂ represents the subdifferential operator in the sense of the convex analysis and Ψ_A denotes the indicator function of the set $A \subset \mathbb{R}$. A similar consideration for the frictional stress leads to

$$-\boldsymbol{\Pi}_\tau \in -\mu \Pi_\nu \partial \|\dot{\boldsymbol{u}}_\tau\| \quad \text{on } \Gamma_3 \times (0, T), \tag{2.12}$$

which is equivalent to (2.9). Finally, (2.10) represents the initial conditions in which $\boldsymbol{u}_0$ and $\boldsymbol{u}_1$ are the initial displacement and velocity, respectively.

2.2. Variational formulation

In order to derive the variational formulation of Problem $\mathcal{P}$, some preliminary material is needed. Throughout this paper the standard notations for Sobolev and Lebesgue spaces associated to Ω and Γ are used. The following spaces are considered

$$V = \{\boldsymbol{v} \in W^{1,s}(\Omega; \mathbb{R}^d) \ : \ \boldsymbol{v} = 0 \ \text{ on } \ \Gamma_1\}, s > 1 \quad H = L^2(\Omega; \mathbb{R}^d).$$

These are real Sobolev spaces endowed with their standard inner products $(\boldsymbol{u}, \boldsymbol{v})_V$ and $(\boldsymbol{\Pi}, \boldsymbol{\tau})_H$ and their associated norms $\|\cdot\|_V$ and $\|\cdot\|_H$, respectively. The duality pairing between V^* and V will be denoted by $\langle \boldsymbol{u}, \boldsymbol{v}\rangle_{V^* \times V}$. We also define $W = \{\boldsymbol{v} \in H^1(\Omega; \mathbb{R}^d) \ : \ \boldsymbol{v} = \mathbf{0} \ \text{ on } \ \Gamma_1\}$. Clearly $V \subset W \subset H \subset W^* \subset V^*$ with all embeddings being continuous.

Note that, for convenience, the Lagrange multipliers λ_ν and λ_τ are taken as equal to $-\Pi_\nu$ and $-\boldsymbol{\Pi}_\tau$, respectively. To this end, we defined by $X_\nu = \left\{ v_\nu|_{\Gamma_3} : \ \boldsymbol{v} \in V \right\}$ and $X_\tau = \left\{ \boldsymbol{v}_\tau|_{\Gamma_3} : \ \boldsymbol{v} \in V \right\}$ the trace spaces equipped with their usual norms. We denote by Y_ν and Y_τ the duals of the spaces X_ν and X_τ, respectively. Moreover, we denote by $\langle \cdot, \cdot \rangle_{Y_\nu, X_\nu}$ and $\langle \cdot, \cdot \rangle_{Y_\tau, X_\tau}$ the corresponding duality pairing mapping. Then a function $\varphi_\nu : X_\nu \to (-\infty, +\infty]$ is introduced, defined by

$$\varphi_\nu(v_\nu) = \int_{\Gamma_3} \Psi_{\mathbb{R}^-}(v_\nu)\, d\Gamma \quad \forall\, v_\nu \in X_\nu.$$

Therefore, the Lagrange multiplier λ_ν related to the contact stress verifies an extended subdifferential inclusion derived from the pointwise subdifferential inclusion defined in (2.11),

$$\lambda_\nu \in \partial \varphi_\nu(u_\nu - g) \quad \text{in} \quad Y_\nu. \tag{2.13}$$

Similarly, we introduce the function $\varphi_\tau : X_\tau \to (-\infty, +\infty]$ defined by

$$\varphi_\tau(\boldsymbol{v}_\tau) = \int_{\Gamma_3} \|\dot{\boldsymbol{v}}_\tau\|\, d\Gamma \quad \forall\, \boldsymbol{v}_\tau \in X_\tau,$$

and, therefore, the condition (2.12) leads to the following extended subdifferential inclusion

$$\boldsymbol{\lambda}_\tau \in \mu \lambda_\nu \partial \varphi_\tau(\boldsymbol{u}_\tau) \quad \text{in} \quad Y_\tau. \tag{2.14}$$

Also, for a regular stress function $\boldsymbol{\Pi}$ the following Green's formula holds:

$$\int_\Omega \boldsymbol{\Pi} : \nabla \boldsymbol{v}\, dx + \int_\Omega \operatorname{Div} \boldsymbol{\Pi} \cdot \boldsymbol{v}\, dx = \int_\Gamma \boldsymbol{\Pi} \boldsymbol{\nu} \cdot \boldsymbol{v}\, da \quad \text{for all } \boldsymbol{v} \in H_1. \tag{2.15}$$

Moreover, in the study of the mechanical problem (2.4)–(2.9) we assume that the body forces and tractions densities have the regularity

$$\boldsymbol{f}_0 \in L^2(0, T; L^{p_1}(\Omega)), \qquad \boldsymbol{f}_1 \in L^2(0, T; L^{p_2}(\Gamma_2)), \tag{2.16}$$

$$\text{where} \quad p_1 \begin{cases} \in (1, \infty) & \text{if } \ d = 2, \\ = \frac{6}{5} & \text{if } \ d = 3, \end{cases} \quad \text{and} \quad p_2 \begin{cases} + \in (1, \infty) & \text{if } \ d = 2, \\ = \frac{4}{3} & \text{if } \ d = 3. \end{cases}$$

Now we turn to the hybrid variational formulation of Problem $\mathcal{P}$. To this end we introduce the element $\boldsymbol{f}$ defined by

$$(\boldsymbol{f}(t), \boldsymbol{v})_V = (\boldsymbol{f}_0(t), \boldsymbol{v})_H + (\boldsymbol{f}_2(t), \boldsymbol{v})_{L^2(\Gamma_2)}, \qquad \forall \boldsymbol{v} \in V. \tag{2.17}$$

By using the duality pairing between V^* and V, Green's formula (2.15) and definition (2.17), we can see

$$\langle \rho \ddot{\boldsymbol{u}}(t), \boldsymbol{v}\rangle_{V^* \times V} + \langle \boldsymbol{\Pi}, \nabla \boldsymbol{v}\rangle_{V^* \times V} = (\boldsymbol{f}(t), \boldsymbol{v})_V + \int_{\Gamma_3} \Pi_\nu v_\nu\, da + \int_{\Gamma_3} \boldsymbol{\Pi}_\tau \cdot \boldsymbol{v}_\tau\, da.$$

Then by using the Lagrange multiplier λ_ν, related to the normal contact stress Π_ν, and the Lagrange multiplier $\boldsymbol{\lambda}_\tau$, related to the tangential contact stress $\boldsymbol{\Pi}_\tau$, we obtain the variational formulation of the frictional contact problem $\mathcal{P}$ in terms of two unknown fields.

We are now in a position to introduce the definition of the weak solution for the considered problem.

Problem $\mathcal{P}_V$. *Find a displacement field* $\boldsymbol{u} \in L^\infty(0,T;V)$ *with* $\dot{\boldsymbol{u}} \in L^2(0,T;W)$ *and* $\ddot{\boldsymbol{u}} \in L^2(0,T;V^*)$, *a normal stress field* $\lambda_\nu : [0,T] \to Y_\nu$ *and a tangential stress field* $\boldsymbol{\lambda}_\tau : [0,T] \to Y_\tau$ *such that* $\forall\, \boldsymbol{v} \in V$

$$\langle \rho \ddot{\boldsymbol{u}}(t), \boldsymbol{v}\rangle_{V^*\times V} + \langle \boldsymbol{\Pi}, \nabla \boldsymbol{v}\rangle_{V^*\times V} + \langle \lambda_\nu(t), v_\nu\rangle_{Y_\nu,X_\nu} + \langle \boldsymbol{\lambda}_\tau(t), \boldsymbol{v}_\tau\rangle_{Y_\tau,X_\tau} = (\boldsymbol{f}(t), \boldsymbol{v})_V, \tag{2.18}$$

$$\lambda_\nu(t) \in \partial\varphi_\nu(u_\nu - g) \quad \text{in } Y_\nu, \tag{2.19}$$

$$\boldsymbol{\lambda}_\tau(t) \in \mu\lambda_\nu \partial\varphi_\tau(\boldsymbol{u}_\tau) \quad \text{in } Y_\tau, \tag{2.20}$$

for all $t \in [0,T]$ *and, moreover,*

$$\boldsymbol{u}(0) = \boldsymbol{u}_0, \qquad \dot{\boldsymbol{u}}(0) = \boldsymbol{u}_1. \tag{2.21}$$

A pair $(\boldsymbol{u}, \lambda)$ which satisfies (2.18), (2.19), (2.20) and the hyper-elastic constitutive law in the form $\boldsymbol{\Pi} = \partial_{\mathbf{F}} W(\mathbf{F})$ is called a *weak solution* to the frictional contact problem $\mathcal{P}_V$. See [27,28] and [31] for further details on the analysis of variational formulation of hyper-elasticity problems.

3. Variational approximation

This section is devoted to the discretization of the variational problem $\mathcal{P}_V$, based on arguments similar to those used in [32–38].

First, we recall some preliminary material concerning the time discretization step. Let N be an integer, let $\Delta t = \frac{T}{N}$ be the time step and define

$$t_n = n\,\Delta t, \quad 0 \le n \le N.$$

Below, for a continuous function $f(t)$ with values in a function space, we use the notation $f_j = f(t_j)$, for $0 \le j \le N$. Finally, for a sequence $\{w_n\}_{n=1}^N$, we denote the midpoint divided differences by

$$\dot{w}_{n-\frac{1}{2}} = (w_n - w_{n-1})/\Delta t = \frac{1}{2}(\dot{w}_n + \dot{w}_{n-1}), \tag{3.1}$$

and, equivalently, we have $\dot{w}_n = -\dot{w}_{n-1} + \frac{2}{\Delta t}(w_n - w_{n-1})$. In the rest of the paper, we use the notation $\square_{n-\frac{1}{2}} = \frac{1}{2}(\square_n + \square_{n-1})$, where $\square_n$ represents the approximation of $\square(t_n)$. Note that the time integration scheme we use is based on the implicit second order midpoint rule given in (3.1).

We now present some material concerning the spatial discretization step. Let Ω be a polygonal domain. Moreover, let $\{\mathcal{T}^h\}$ be a regular family of triangular finite element partitions of $\overline{\Omega}$ that are compatible with the boundary decomposition $\overline{\Gamma} = \overline{\Gamma_1} \cup \overline{\Gamma_2} \cup \overline{\Gamma_3}$, i.e., if one side of an element $Tr \in \mathcal{T}^h$ has more than one point on Γ, then the side lies entirely on $\overline{\Gamma_1}$, $\overline{\Gamma_2}$ or $\overline{\Gamma_3}$. The space V is approximated by the finite dimensional space $V^h \subset V$ of continuous and piecewise affine functions, that is,

$$V^h = \{\, \boldsymbol{v}^h \in [C(\overline{\Omega})]^d \;:\; \boldsymbol{v}^h|_{Tr} \in [P_1(Tr)]^d \;\; \forall\, Tr \in \mathcal{T}^h,$$
$$\boldsymbol{v}^h = \mathbf{0} \text{ at the nodes on } \Gamma_1 \,\},$$

where $P_1(Tr)$ represents the space of polynomials of degree less or equal to one in Tr and $h > 0$ denotes the spatial discretization parameter. For the discretization of the Lagrange multiplier spaces Y_ν and Y_τ, we use discontinuous piecewise constant functions as it is done in [39]. The discrete Lagrange multiplier spaces are denoted by Y_ν^h and Y_τ^h.

More details about the discretization step can be found in [12,37,38].

Let $\boldsymbol{u}_0^h \in V^h$ and $\boldsymbol{u}_1^h \in V^h$ be finite element approximations of $\boldsymbol{u}_0$ and $\boldsymbol{u}_1$, respectively. Then, using the previous notations, the midpoint scheme (3.1) and time approximation for the discretization of the tangential velocity $\dot{\boldsymbol{u}}_\tau(t)$ given by $\dot{\boldsymbol{u}}_{\tau\,n-\frac{1}{2}} = (\boldsymbol{u}_{\tau n} - \boldsymbol{u}_{\tau n-1})/\Delta t$, it leads to the following fully discrete approximation of the Problem $\mathcal{P}_V$ at the time $t_{n-\frac{1}{2}}$

Problem $\mathcal{P}_V^{h\Delta t}$. *Find a discrete displacement field* $\boldsymbol{u}^{h\Delta t} = \{\boldsymbol{u}_n^{h\Delta t}\}_{n=0}^N \subset V^h$, *a discrete normal stress field* $\lambda_\nu^{h\Delta t} = \{\lambda_{\nu\,n}^{h\Delta t}\}_{n=0}^N \subset Y_\nu^h$ *and a discrete tangential stress field* $\boldsymbol{\lambda}_\tau^{h\Delta t} = \{\boldsymbol{\lambda}_{\tau\,n}^{h\Delta t}\}_{n=0}^N \subset Y_\tau^h$ *such that, for all* $n = 1, \ldots, N$,

$$\langle \rho \ddot{\boldsymbol{u}}_{n-\frac{1}{2}}^{h\Delta t}, \boldsymbol{v}^h\rangle_{V^*\times V} + \langle \boldsymbol{\Pi}, \nabla \boldsymbol{v}^h\rangle_{V^*\times V} + \langle \lambda_{\nu\,n-\frac{1}{2}}^{h\Delta t}, v_\nu^h\rangle_{Y_\nu^h,X_\nu^h} + \langle \boldsymbol{\lambda}_{\tau\,n-\frac{1}{2}}^{h\Delta t}, \boldsymbol{v}_\tau^h\rangle_{Y_\tau^h,X_\tau^h}$$
$$= \langle \boldsymbol{f}_{n-\frac{1}{2}}^{h\Delta t}, \boldsymbol{v}^h\rangle_{V^*\times V} \quad \forall\, \boldsymbol{v} \in V^h, \tag{3.2}$$

$$-\lambda_{\nu\,n-\frac{1}{2}}^{h\Delta t} \in \partial\varphi_\nu(u_{\nu\,n-\frac{1}{2}}^{h\Delta t} - g), \tag{3.3}$$

$$-\boldsymbol{\lambda}_{\tau\,n-\frac{1}{2}}^{h\Delta t} \in -\mu\lambda_{\nu\,n-\frac{1}{2}}^{h\Delta t} \partial\varphi_\tau(\dot{\boldsymbol{u}}_{\tau\,n-\frac{1}{2}}^{h\Delta t}), \tag{3.4}$$

$$\boldsymbol{u}_0^{h\Delta t} = \boldsymbol{u}_0^h, \qquad \delta \boldsymbol{u}_0^{h\Delta t} = \boldsymbol{u}_1^h. \tag{3.5}$$

Where $\ddot{\boldsymbol{u}}_{n-\frac{1}{2}}^{h\Delta t} = \frac{\dot{\boldsymbol{u}}_n^{h\Delta t} - \dot{\boldsymbol{u}}_{n-1}^{h\Delta t}}{\Delta t}$ is the midpoint time approximation of the acceleration $\ddot{\boldsymbol{u}}$ at the time $t_{n-\frac{1}{2}}$.

Starting from the Problem $\mathcal{P}_V^{h\Delta t}$ and using the formalism introduced in [40] and [9] based on the Galerkin approximation for hyper-elasticity, we will directly pose the elementary discrete strong problem as follows.

Problem $\mathcal{P}_S^{nodal}$. *Find a global displacement vector $\boldsymbol{u}^{\Delta t} = \{\boldsymbol{u}_n^{\Delta t}\}_{n=0}^N$, a global normal stress vector $\lambda_\nu^{\Delta t} = \{\lambda_{\nu n}^{\Delta t}\}_{n=0}^N$ and a global tangential stress vector $\boldsymbol{\lambda}_\tau^{\Delta t} = \{\boldsymbol{\lambda}_{\tau n}^{\Delta t}\}_{n=0}^N$ such that, for all $n = 1$*

$$\begin{aligned}
&\rho \ddot{\boldsymbol{u}}_{n-\frac{1}{2}}^{\Delta t} + A(\boldsymbol{u}_{n-\frac{1}{2}}^{\Delta t}) + \lambda_{\nu\, n-\frac{1}{2}}^{\Delta t} \boldsymbol{\nu} + \boldsymbol{\lambda}_{\tau\, n-\frac{1}{2}}^{\Delta t} - \boldsymbol{f} = \boldsymbol{0}\\
&-\lambda_{\nu\, n-\frac{1}{2}}^{\Delta t} \in \partial \varphi_\nu(u_{\nu\, n-\frac{1}{2}}^{\Delta t} - g),\\
&-\boldsymbol{\lambda}_{\tau\, n-\frac{1}{2}}^{\Delta t} \in -\mu \lambda_{\nu\, n-\frac{1}{2}}^{\Delta t} \partial \varphi_\tau(\dot{\boldsymbol{u}}_{\tau\, n-\frac{1}{2}}^{\Delta t}),\\
&\boldsymbol{u}_0^{\Delta t} = \boldsymbol{u}_0, \qquad \delta \boldsymbol{u}_0^{\Delta t} = \boldsymbol{u}_1.
\end{aligned}$$

where $A(.)$ is the internal force vector coming from the first Piola–Kirchhoff tensor Π.

In the rest of the paper, to simplify the notation and the readability, we do not indicate the dependence of various variables with respect to the discretization parameters Δt and h, i.e., for example, we write $\boldsymbol{u}$ instead of $\boldsymbol{u}_{n-\frac{1}{2}}^{h\Delta t}$.

4. Frictionless unilateral contact law with a gap

At first, we consider a frictionless unilateral contact law with a gap. Denoting by p the index of the vertices on $\Gamma_3^h \in \Gamma_3$ and with these considerations, the discrete unilateral conditions verified on the contact boundary Γ_3^h are given by

$$u_{\nu,p} \leq g, \tag{4.1}$$

$$\lambda_{\nu,p} \geq 0, \tag{4.2}$$

$$(u_{\nu,p} - g)\lambda_{\nu,p} = 0, \tag{4.3}$$

$$\boldsymbol{\lambda}_{\tau,p} = \boldsymbol{0}. \tag{4.4}$$

The discrete Signorini conditions (4.1)–(4.3) are represented by the following nonlinear complementary function $\mathcal{R}_\nu^\lambda(u_{\nu,p}, \lambda_{\nu,p}) = 0$

$$\mathcal{R}_\nu^\lambda(u_{\nu,p}, \lambda_{\nu,p}) = \lambda_{\nu,p} - \max(0, \lambda_{\nu,p} + c_\nu(u_{\nu,p} - g)). \tag{4.5}$$

Such a result was already proved in [26]. Now, we recall the generalized derivative of the complementary function in the gap and contact cases.

Gap case: $\lambda_{\nu,p} + c_\nu(u_{\nu,p} - g) \leq 0$

$$\mathcal{R}_\nu^\lambda(u_{\nu,p}, \lambda_{\nu,p}) = \lambda_{\nu,p}.$$

Then, it is obvious to see that

$$d_{u_{\nu,p}} \mathcal{R}_\nu^\lambda = 0, \tag{4.6}$$

$$d_{\lambda_{\nu,p}} \mathcal{R}_\nu^\lambda = d\lambda_{\nu,p}. \tag{4.7}$$

Contact case: $\lambda_{\nu,p} + c_\nu(u_{\nu,p} - g) > 0$

$$\mathcal{R}_\nu^\lambda(u_{\nu,p}, \lambda_{\nu,p}) = -c_\nu(u_{\nu,p} - g).$$

Then

$$d_{u_{\nu,p}} \mathcal{R}_\nu^\lambda = -c_\nu du_{\nu,p}, \tag{4.8}$$

$$d_{\lambda_{\nu,p}} \mathcal{R}_\nu^\lambda = 0. \tag{4.9}$$

By combining (4.6) and (4.9) with $\mathcal{G}_{\mathcal{R}_\nu^\lambda}$ the generalized derivative of $\mathcal{R}_\nu^\lambda$, we obtain

$$\mathcal{G}_{\mathcal{R}_\nu^\lambda}(u_{\nu,p}, \lambda_{\nu,p})(\delta u_{\nu,p}, \delta\lambda_{\nu,p}) = -c_\nu(1 - \chi_{Gap})\delta u_{\nu,p} + \chi_{Gap}\delta\lambda_{\nu,p}, \tag{4.10}$$

where

$$\begin{aligned}
&\chi_{Gap} = 1, \text{ if } \lambda_{\nu,p} + c_\nu(u_{\nu,p} - g) \leq 0,\\
&\chi_{Gap} = 0, \text{ if } \lambda_{\nu,p} + c_\nu(u_{\nu,p} - g) > 0.
\end{aligned}$$

Using now the semismooth Newton formalism at the current $(u_{\nu,p}^{(k)}, \lambda_{\nu,p}^{(k)})$, one can derive the new iterate $(u_{\nu,p}^{(k+1)}, \lambda_{\nu,p}^{(k+1)})$ by the following iterative scheme of index k:

$$\mathcal{G}_{\mathcal{R}_\nu^\lambda}(u_{\nu,p}^{(k)}, \lambda_{\nu,p}^{(k)})(\delta u_{\nu,p}^{(k+1)}, \delta\lambda_{\nu,p}^{(k+1)}) = -\mathcal{R}_\nu^\lambda(u_{\nu,p}^{(k)}, \lambda_{\nu,p}^{(k)}), \tag{4.11}$$

$$\text{where} \quad (u_{\nu,p}^{(k+1)}, \lambda_{\nu,p}^{(k+1)}) = (u_{\nu,p}^{(k)}, \lambda_{\nu,p}^{(k)}) + (\delta u_{\nu,p}^{(k+1)}, \delta\lambda_{\nu,p}^{(k+1)}) \tag{4.12}$$

Gap case: $\mathcal{X}_{Gap} = 1$

$$\lambda_{\nu,p}^{(k+1)} - \lambda_{\nu,p}^{(k)} = -\lambda_{\nu,p}^{(k)}. \tag{4.13}$$

Next,

$$\lambda_{\nu,p}^{(k+1)} = 0, \tag{4.14}$$

Contact case: $\mathcal{X}_{Gap} = 0$

$$-c_\nu(u_{\nu,p}^{(k+1)} - u_{\nu,p}^{(k)}) = c_\nu(u_{\nu,p}^{(k)} - g). \tag{4.15}$$

Next,

$$u_{\nu,p}^{(k+1)} = g. \tag{4.16}$$

Let us denote by $\mathcal{S}$ the set of all nodes of the finite element mesh belonging to Γ_3^h and p the index of a node belonging to $\mathcal{S}$.

Primal–Dual Active Set (PDAS) method

In the following, we use the same notations as in [21]. The discrete contact conditions (4.1)–(4.3) are realized by applying an active set strategy on the nonlinear complementary function $\mathcal{R}_\nu^\lambda$ based on a Newton semi-smooth iterative scheme. The active and inactive sets are defined as follows

$$\mathcal{A}_\nu^{k+1} = \{p \in \mathcal{S} : \lambda_{\nu,p}^{(k)} + c_\nu(u_{\nu,p}^{(k)} - g) > 0\},$$
$$\mathcal{I}_\nu^{k+1} = \{p \in \mathcal{S} : \lambda_{\nu,p}^{(k)} + c_\nu(u_{\nu,p}^{(k)} - g) \leq 0\}, .$$

The status of a given node at the iteration k depends on the set it belongs to; it can be either in the non-contact (gap) or contact status.

At each increment n corresponding to the time $t_{n-\frac{1}{2}}$, we also introduce the global nonlinear complementary operator $\mathcal{R}(.,.) = \left(\mathcal{R}^{\boldsymbol{u}}(.,.), \mathcal{R}_\nu^\lambda(.,.), \mathcal{R}_\tau^\lambda(.,.)\right)$ which describes the system of nonlinear equations arising from the discretized problem $\mathcal{P}_S^{nodal}$ in the case of frictionless unilateral contact, and defined by

$$\mathcal{R}(\boldsymbol{u}, \boldsymbol{\lambda}) = \begin{pmatrix} \mathcal{R}^{\boldsymbol{u}}(\boldsymbol{u}, \boldsymbol{\lambda}) = \rho\ddot{\boldsymbol{u}} + A(\boldsymbol{u}) + \lambda_\nu \boldsymbol{\nu} - \boldsymbol{f} \\ \mathcal{R}_\nu^\lambda(\boldsymbol{u}, \boldsymbol{\lambda}) = \lambda_{\nu,p} - \max(0, \lambda_{\nu,p} + c_\nu(u_{\nu,p} - g)) \\ \mathcal{R}_\tau^\lambda(\boldsymbol{u}, \boldsymbol{\lambda}) = \boldsymbol{0} \end{pmatrix} = \boldsymbol{0}.$$

Now, we turn to the description of the iterative active set algorithm of index k.

(i) Choose $(\boldsymbol{u}^{(0)}, \boldsymbol{\lambda}^{(0)})$, $c_\nu > 0$ and set $k = 0$.

(ii) Set the active and inactive sets:

$$\mathcal{A}_\nu^{k+1} = \{p \in \mathcal{S} : \lambda_{\nu,p}^{(k)} + c_\nu(u_{\nu,p}^{(k)} - g) > 0\},$$
$$\mathcal{I}_\nu^{k+1} = \mathcal{S} \setminus \mathcal{A}_\nu^{k+1}.$$

(iii) Find $(\boldsymbol{u}^{(k+1)}, \boldsymbol{\lambda}^{(k+1)})$ such that

$$\rho\ddot{\boldsymbol{u}}^{(k+1)} + A(\boldsymbol{u}^{(k+1)}) + \lambda_\nu^{(k+1)}\boldsymbol{\nu} = \boldsymbol{f}, \tag{4.17}$$

$$u_{\nu,p}^{(k+1)} = g \quad \text{for all} \quad p \in \mathcal{A}_\nu^{k+1}, \tag{4.18}$$

$$\lambda_{\nu,p}^{(k+1)} = 0 \quad \text{for all} \quad p \in \mathcal{I}_\nu^{k+1}. \tag{4.19}$$

(iv) If $\|(\boldsymbol{u}^{(k+1)}, \boldsymbol{\lambda}^{(k+1)}) - (\boldsymbol{u}^{(k)}, \boldsymbol{\lambda}^{(k)})\| \leq \epsilon$, $\|\mathcal{R}(\boldsymbol{u}^{(k+1)}, \boldsymbol{\lambda}^{(k+1)})\| \leq \epsilon$, $\mathcal{A}_\nu^{k+1} = \mathcal{A}_\nu^k$ then stop, else goto (ii).

Remark. The nonlinear system (4.17) corresponding to $\mathcal{R}^{\boldsymbol{u}}(\boldsymbol{u}^{(k+1)}, \boldsymbol{\lambda}^{(k+1)}) = \boldsymbol{0}$ has to be solved by a Newton method at each active set iteration.

5. Bilateral case with Tresca's law of friction

In this section only, we consider a bilateral contact condition combined with a Tresca's law of friction.

Denoting by p the index of the vertices on $\Gamma_3^h \in \Gamma_3$ and with these considerations, the discrete conditions verified on the contact boundary are given by

$$u_{\nu,p} = 0, \tag{5.1}$$

$$\begin{cases} \|\boldsymbol{\lambda}_{\tau,p}\| \leq S, \\ \|\boldsymbol{\lambda}_{\tau,p}\| < S \Longrightarrow \dot{\boldsymbol{u}}_{\tau,p} = 0, \\ \|\boldsymbol{\lambda}_{\tau,p}\| = S \Longrightarrow \exists \beta \geq 0 : \boldsymbol{\lambda}_{\tau,p} = \beta \dot{\boldsymbol{u}}_{\tau,p}, \end{cases} \tag{5.2}$$

where $S > 0$ is the Tresca's friction threshold fixed. In order to derive the iterative scheme, we introduce a nonlinear complementary function $\mathcal{R}_\tau^\lambda(\dot{\boldsymbol{u}}_{\tau,p}, \boldsymbol{\lambda}_{\tau,p}) = 0$ defined by

$$\mathcal{R}_\tau^\lambda(\dot{\boldsymbol{u}}_{\tau,p}, \boldsymbol{\lambda}_{\tau,p}) = \max(S, \|\boldsymbol{\lambda}_{\tau,p} + c_\tau \dot{\boldsymbol{u}}_{\tau,p}\|)\boldsymbol{\lambda}_{\tau,p} - S(\boldsymbol{\lambda}_{\tau,p} + c_\tau \dot{\boldsymbol{u}}_{\tau,p}). \tag{5.3}$$

Let us prove this result.

Proposition 5.1. *Let $c_\tau > 0$, the Tresca's friction conditions (5.2) are equivalent to $\mathcal{R}_\tau^\lambda(\dot{\boldsymbol{u}}_{\tau,p}, \boldsymbol{\lambda}_{\tau,p}) = 0$.*

Proof. Let us assume that (5.2) hold. Then, either $\|\boldsymbol{\lambda}_{\tau,p}\| < S$ or $\|\boldsymbol{\lambda}_{\tau,p}\| = S$. First, if $\|\boldsymbol{\lambda}_{\tau,p}\| < S$, it implies that $\dot{\boldsymbol{u}}_{\tau,p} = 0$. So

$$\mathcal{R}_\tau^\lambda(\dot{\boldsymbol{u}}_{\tau,p}, \boldsymbol{\lambda}_{\tau,p}) = \max(S, \|\boldsymbol{\lambda}_{\tau,p}\|)\boldsymbol{\lambda}_{\tau,p} - S(\boldsymbol{\lambda}_{\tau,p}) = 0. \tag{5.4}$$

Suppose now that $\|\boldsymbol{\lambda}_{\tau,p}\| = S$ and $\boldsymbol{\lambda}_{\tau,p} = \beta \dot{\boldsymbol{u}}_{\tau,p}$ with $\beta > 0$; therefore

$$\mathcal{R}_\tau^\lambda(\dot{\boldsymbol{u}}_{\tau,p}, \boldsymbol{\lambda}_{\tau,p}) = \max(S, (\beta + c_\tau)\|\dot{\boldsymbol{u}}_{\tau,p}\|)\beta \dot{\boldsymbol{u}}_{\tau,p} - \beta \|\dot{\boldsymbol{u}}_{\tau,p}\|(\beta + c_\tau)\dot{\boldsymbol{u}}_{\tau,p} = 0. \tag{5.5}$$

Conversely, assume now that $\mathcal{R}_\tau^\lambda(\dot{\boldsymbol{u}}_{\tau,p}, \boldsymbol{\lambda}_{\tau,p}) = 0$ holds; depending on the value of $\boldsymbol{\lambda}_{\tau,p}$ and $\dot{\boldsymbol{u}}_{\tau,p}$, one can have

$$S = \max(S, \|\boldsymbol{\lambda}_{\tau,p} + c_\tau \dot{\boldsymbol{u}}_{\tau,p}\|), \tag{5.6}$$

$$\|\boldsymbol{\lambda}_{\tau,p} + c_\tau \dot{\boldsymbol{u}}_{\tau,p}\| = \max(S, \|\boldsymbol{\lambda}_{\tau,p} + c_\tau \dot{\boldsymbol{u}}_{\tau,p}\|). \tag{5.7}$$

By combining (5.3) and (5.6), we get

$$S\boldsymbol{\lambda}_{\tau,p} = S(\boldsymbol{\lambda}_{\tau,p} + c_\tau \dot{\boldsymbol{u}}_{\tau,p}), \tag{5.8}$$

which means that $\dot{\boldsymbol{u}}_{\tau,p} = 0$, since $c_\tau > 0$, and therefore (from (5.6)) $S > \|\boldsymbol{\lambda}_{\tau,p}\|$. At last, we combine (5.3) and (5.7) to obtain

$$\|\boldsymbol{\lambda}_{\tau,p} + c_\tau \dot{\boldsymbol{u}}_{\tau,p}\|\boldsymbol{\lambda}_{\tau,p} = S(\boldsymbol{\lambda}_{\tau,p} + c_\tau \dot{\boldsymbol{u}}_{\tau,p}). \tag{5.9}$$

Note that $\|\boldsymbol{\lambda}_{\tau,p} + c_\tau \dot{\boldsymbol{u}}_{\tau,p}\| \geq S > 0$. We get $\|\boldsymbol{\lambda}_{\tau,p}\| = S$. Also, it is trivial that

$$\boldsymbol{\lambda}_{\tau,p} = \frac{Sc_\tau}{\|\boldsymbol{\lambda}_{\tau,p} + c_\tau \dot{\boldsymbol{u}}_{\tau,p}\| - S} \dot{\boldsymbol{u}}_{\tau,p}. \tag{5.10}$$

Let $\beta = \frac{Sc_\tau}{\|\boldsymbol{\lambda}_{\tau,p} + c_\tau \dot{\boldsymbol{u}}_{\tau,p}\| - S}$. With (5.7), it is clear that $\beta > 0$, which concludes the proof. A similar proof is available in [18]. □

Now, we compute the generalized derivative of $\mathcal{R}_\tau^\lambda(\cdot, \cdot)$ in the stick and slip cases

Stick case: $\|\boldsymbol{\lambda}_{\tau,p} + c_\tau \dot{\boldsymbol{u}}_{\tau,p}\| \leq S$

$$\mathcal{R}_\tau^\lambda(\dot{\boldsymbol{u}}_{\tau,p}, \boldsymbol{\lambda}_{\tau,p}) = -Sc_\tau \dot{\boldsymbol{u}}_{\tau,p}.$$

By definition

$$d_{\dot{\boldsymbol{u}}_{\tau,p}} \mathcal{R}_\tau^\lambda = \frac{\partial \mathcal{R}_\tau^\lambda}{\partial \dot{\boldsymbol{u}}_{\tau,p}} d\dot{\boldsymbol{u}}_{\tau,p},$$

$$d_{\boldsymbol{\lambda}_{\tau,p}} \mathcal{R}_\tau^\lambda = \frac{\partial \mathcal{R}_\tau^\lambda}{\partial \boldsymbol{\lambda}_{\tau,p}} d\boldsymbol{\lambda}_{\tau,p}.$$

and then

$$d_{\dot{\boldsymbol{u}}_{\tau,p}} \mathcal{R}_\tau^\lambda = -Sc_\tau d\dot{\boldsymbol{u}}_{\tau,p}, \tag{5.11}$$

$$d_{\boldsymbol{\lambda}_{\tau,p}} \mathcal{R}_\tau^\lambda = 0. \tag{5.12}$$

Slip case: $\|\boldsymbol{\lambda}_{\tau,p} + c_\tau \dot{\boldsymbol{u}}_{\tau,p}\| > S$

$$\mathcal{R}_\tau^\lambda(\dot{\boldsymbol{u}}_{\tau,p}, \boldsymbol{\lambda}_{\tau,p}) = \|\boldsymbol{\lambda}_{\tau,p} + c_\tau \dot{\boldsymbol{u}}_{\tau,p}\|\boldsymbol{\lambda}_{\tau,p} - S(\boldsymbol{\lambda}_{\tau,p} + c_\tau \dot{\boldsymbol{u}}_{\tau,p}).$$

We get

$$d_{\dot{\boldsymbol{u}}_{\tau,p}}\mathcal{R}_\tau^\lambda = \Big(c_\tau \boldsymbol{\lambda}_{\tau,p}\frac{(\boldsymbol{\lambda}_{\tau,p}+c_\tau\dot{\boldsymbol{u}}_{\tau,p})^T}{\|\boldsymbol{\lambda}_{\tau,p}+c_\tau\dot{\boldsymbol{u}}_{\tau,p}\|} - Sc_\tau \boldsymbol{I}_2\Big)d\dot{\boldsymbol{u}}_{\tau,p}, \tag{5.13}$$

$$d_{\boldsymbol{\lambda}_{\tau,p}}\mathcal{R}_\tau^\lambda = \Big(\boldsymbol{\lambda}_{\tau,p}\frac{(\boldsymbol{\lambda}_{\tau,p}+c_\tau\dot{\boldsymbol{u}}_{\tau,p})^T}{\|\boldsymbol{\lambda}_{\tau,p}+c_\tau\dot{\boldsymbol{u}}_{\tau,p}\|} + \|\boldsymbol{\lambda}_{\tau,p}+c_\tau\dot{\boldsymbol{u}}_{\tau,p}\|\boldsymbol{I}_2 - S\boldsymbol{I}_2\Big)d\boldsymbol{\lambda}_{\tau,p}. \tag{5.14}$$

By combining (5.11)–(5.14), with $\mathcal{G}_{\mathcal{R}_\tau^\lambda}$ the generalized derivative of $\mathcal{R}_\tau^\lambda$, we obtain

$$\mathcal{G}_{\mathcal{R}_\tau^\lambda}(\dot{\boldsymbol{u}}_{\tau,p},\boldsymbol{\lambda}_{\tau,p})(\delta\dot{\boldsymbol{u}}_{\tau,p},\delta\boldsymbol{\lambda}_{\tau,p}) = \mathcal{X}_{Slip}\boldsymbol{\lambda}_{\tau,p}\frac{(\boldsymbol{\lambda}_{\tau,p}+c_\tau\dot{\boldsymbol{u}}_{\tau,p})^T}{\|\boldsymbol{\lambda}_{\tau,p}+c_\tau\dot{\boldsymbol{u}}_{\tau,p}\|}(\delta\boldsymbol{\lambda}_{\tau,p}+c_\tau\delta\dot{\boldsymbol{u}}_{\tau,p}) \tag{5.15}$$

$$-S(\mathcal{X}_{Slip}\delta\boldsymbol{\lambda}_{\tau,p}+c_\tau\delta\dot{\boldsymbol{u}}_{\tau,p}) + \mathcal{X}_{Slip}\|\boldsymbol{\lambda}_{\tau,p}+c_\tau\dot{\boldsymbol{u}}_{\tau,p}\|\delta\boldsymbol{\lambda}_{\tau,p} \tag{5.16}$$

where

$$\mathcal{X}_{Slip} = 0, \text{ if } \|\boldsymbol{\lambda}_{\tau,p}+c_\tau\dot{\boldsymbol{u}}_{\tau,p}\| \le S \tag{5.17}$$

$$\mathcal{X}_{Slip} = 1, \text{ if } \|\boldsymbol{\lambda}_{\tau,p}+c_\tau\dot{\boldsymbol{u}}_{\tau,p}\| > S. \tag{5.18}$$

Using now the semismooth Newton formalism at the current $(\dot{\boldsymbol{u}}_{\tau,p}^{(k)}, \boldsymbol{\lambda}_{\tau,p}^{(k)})$, one can derive the new iterate $(\dot{\boldsymbol{u}}_{\tau,p}^{(k+1)}, \boldsymbol{\lambda}_{\tau,p}^{(k+1)})$

$$\mathcal{G}_{\mathcal{R}_\tau^\lambda}(\dot{\boldsymbol{u}}_{\tau,p}^{(k)},\boldsymbol{\lambda}_{\tau,p}^{(k)})(\delta\boldsymbol{u}_{\tau,p}^{(k+1)},\delta\boldsymbol{\lambda}_{\tau,p}^{(k+1)}) = -\mathcal{R}_\tau^\lambda(\dot{\boldsymbol{u}}_{\tau,p}^{(k)},\boldsymbol{\lambda}_{\tau,p}^{(k)}) \tag{5.19}$$

$$(\dot{\boldsymbol{u}}_{\tau,p}^{(k+1)},\boldsymbol{\lambda}_{\tau,p}^{(k+1)}) = (\dot{\boldsymbol{u}}_{\tau,p}^{(k)},\boldsymbol{\lambda}_{\tau,p}^{(k)}) + (\delta\dot{\boldsymbol{u}}_{\tau,p}^{(k+1)},\delta\boldsymbol{\lambda}_{\tau,p}^{(k+1)}) \tag{5.20}$$

Stick case: $\mathcal{X}_{Slip} = 0$

$$-Sc_\tau(\dot{\boldsymbol{u}}_{\tau,p}^{(k+1)} - \dot{\boldsymbol{u}}_{\tau,p}^{(k)}) = Sc_\tau\dot{\boldsymbol{u}}_{\tau,p}^{(k)} \tag{5.21}$$

and then, since $Sc_\tau > 0$

$$\dot{\boldsymbol{u}}_{\tau,p}^{(k+1)} = 0 \tag{5.22}$$

Slip case: $\mathcal{X}_{Slip} = 1$

$$\begin{aligned}
&\Big(c_\tau\boldsymbol{\lambda}_{\tau,p}^{(k)}\frac{(\boldsymbol{\lambda}_{\tau,p}^{(k)}+c_\tau\dot{\boldsymbol{u}}_{\tau,p}^{(k)})^T}{\|\boldsymbol{\lambda}_{\tau,p}^{(k)}+c_\tau\dot{\boldsymbol{u}}_{\tau,p}^{(k)}\|} - Sc_\tau\boldsymbol{I}_2\Big)(\dot{\boldsymbol{u}}_{\tau,p}^{(k+1)} - \dot{\boldsymbol{u}}_{\tau,p}^{(k)})\\
&+\Big(\boldsymbol{\lambda}_{\tau,p}^{(k)}\frac{(\boldsymbol{\lambda}_{\tau,p}^{(k)}+c_\tau\dot{\boldsymbol{u}}_{\tau,p}^{(k)})^T}{\|\boldsymbol{\lambda}_{\tau,p}^{(k)}+c_\tau\dot{\boldsymbol{u}}_{\tau,p}^{(k)}\|} - S\boldsymbol{I}_2 + \|\boldsymbol{\lambda}_{\tau,p}^{(k)}+c_\tau\dot{\boldsymbol{u}}_{\tau,p}^{(k)}\|\boldsymbol{I}_2\Big)(\boldsymbol{\lambda}_{\tau,p}^{(k+1)} - \boldsymbol{\lambda}_{\tau,p}^{(k)})\\
&= -\|\boldsymbol{\lambda}_{\tau,p}^{(k)}+c_\tau\dot{\boldsymbol{u}}_{\tau,p}^{(k)}\|\boldsymbol{\lambda}_{\tau,p}^{(k)} + S(\boldsymbol{\lambda}_{\tau,p}^{(k)}+c_\tau\dot{\boldsymbol{u}}_{\tau,p}^{(k)}).
\end{aligned}$$

and then

$$\begin{aligned}
&\Big(c_\tau\boldsymbol{\lambda}_{\tau,p}^{(k)}\frac{(\boldsymbol{\lambda}_{\tau,p}^{(k)}+c_\tau\dot{\boldsymbol{u}}_{\tau,p}^{(k)})^T}{\|\boldsymbol{\lambda}_{\tau,p}^{(k)}+c_\tau\dot{\boldsymbol{u}}_{\tau,p}^{(k)}\|} - Sc_\tau\boldsymbol{I}_2\Big)\dot{\boldsymbol{u}}_{\tau,p}^{(k+1)} - c_\tau\boldsymbol{\lambda}_{\tau,p}^{(k)}\frac{(\boldsymbol{\lambda}_{\tau,p}^{(k)}+c_\tau\dot{\boldsymbol{u}}_{\tau,p}^{(k)})^T}{\|\boldsymbol{\lambda}_{\tau,p}^{(k)}+c_\tau\dot{\boldsymbol{u}}_{\tau,p}^{(k)}\|}\dot{\boldsymbol{u}}_{\tau,p}^{(k)}\\
&+\Big(\boldsymbol{\lambda}_{\tau,p}^{(k)}\frac{(\boldsymbol{\lambda}_{\tau,p}^{(k)}+c_\tau\dot{\boldsymbol{u}}_{\tau,p}^{(k)})^T}{\|\boldsymbol{\lambda}_{\tau,p}^{(k)}+c_\tau\dot{\boldsymbol{u}}_{\tau,p}^{(k)}\|} - S\boldsymbol{I}_2 + \|\boldsymbol{\lambda}_{\tau,p}^{(k)}+c_\tau\dot{\boldsymbol{u}}_{\tau,p}^{(k)}\|\boldsymbol{I}_2\Big)\boldsymbol{\lambda}_{\tau,p}^{(k+1)} - \boldsymbol{\lambda}_{\tau,p}^{(k)}\frac{(\boldsymbol{\lambda}_{\tau,p}^{(k)}+c_\tau\dot{\boldsymbol{u}}_{\tau,p}^{(k)})^T}{\|\boldsymbol{\lambda}_{\tau,p}^{(k)}+c_\tau\dot{\boldsymbol{u}}_{\tau,p}^{(k)}\|}\boldsymbol{\lambda}_{\tau,p}^{(k)}\\
&= 0
\end{aligned}$$

At this point, for the sake of clarity, let

$$\boldsymbol{F}^{(k)} = \boldsymbol{\lambda}_{\tau,p}^{(k)}\frac{(\boldsymbol{\lambda}_{\tau,p}^{(k)}+c_\tau\dot{\boldsymbol{u}}_{\tau,p}^{(k)})^T}{\|\boldsymbol{\lambda}_{\tau,p}^{(k)}+c_\tau\dot{\boldsymbol{u}}_{\tau,p}^{(k)}\|},$$

$$E^{(k)} = \frac{1}{\|\boldsymbol{\lambda}_{\tau,p}^{(k)}+c_\tau\dot{\boldsymbol{u}}_{\tau,p}^{(k)}\|}.$$

With these notations, one can write

$$c_\tau E^{(k)}\Big(\boldsymbol{F}^{(k)} - S\boldsymbol{I}_2\Big)\dot{\boldsymbol{u}}_{\tau,p}^{(k+1)} + \Big(E^{(k)}(\boldsymbol{F}^{(k)} - S\boldsymbol{I}_2) + \boldsymbol{I}_2\Big)\boldsymbol{\lambda}_{\tau,p}^{(k+1)} = E^{(k)}\boldsymbol{F}^{(k)}\Big(\boldsymbol{\lambda}_{\tau,p}^{(k)} + c_\tau\dot{\boldsymbol{u}}_{\tau,p}^{(k)}\Big).$$

Now, let

$$\boldsymbol{M}_p^{(k)} = E^{(k)}(\boldsymbol{F}^{(k)} - S\boldsymbol{I}_2),$$

$$\boldsymbol{h}_p^{(k)} = E^{(k)}\boldsymbol{F}^{(k)}\Big(\boldsymbol{\lambda}_{\tau,p}^{(k)} + c_\tau\dot{\boldsymbol{u}}_{\tau,p}^{(k)}\Big).$$

Then

$$c_\tau \boldsymbol{M}_p^{(k)} \dot{\boldsymbol{u}}_{\tau,p}^{(k+1)} + \left(\boldsymbol{M}_p^{(k)} + \boldsymbol{I}_2\right)\boldsymbol{\lambda}_{\tau,p}^{(k+1)} = \boldsymbol{h}_p^{(k)}.$$

In order to simplify even further the notations, we introduce the following operators:

$$\boldsymbol{L}_p^{(k)} = c_\tau(\boldsymbol{I}_2 + \boldsymbol{M}_p^{(k)})^{-1}\boldsymbol{M}_p^{(k)},$$
$$\boldsymbol{r}_p^{(k)} = (\boldsymbol{I}_2 + \boldsymbol{M}_p^{(k)})^{-1}\boldsymbol{h}_p^{(k)}.$$

And, at last

$$\boldsymbol{L}_p^{(k)} \dot{\boldsymbol{u}}_{\tau,p}^{(k+1)} + \boldsymbol{\lambda}_{\tau,p}^{(k+1)} = \boldsymbol{r}_p^{(k)}. \tag{5.23}$$

Let us denote by $\mathcal{S}$ the set of all nodes of the finite element mesh belonging to Γ_3^h and p the index of a node belonging to $\mathcal{S}$. At each increment n for the time $t_{n-\frac{1}{2}}$, we also introduce the operator $\mathcal{R}$ which describes the system of nonlinear equations arising from the discretized problem $\mathcal{P}_S^{nodal}$ in the case of bilateral contact and Tresca friction, and defined by

$$\mathcal{R}(\boldsymbol{u}, \boldsymbol{\lambda}) = \begin{pmatrix} \mathcal{R}^{\boldsymbol{u}}(\boldsymbol{u}, \boldsymbol{\lambda}) = \rho\ddot{\boldsymbol{u}} + A(\boldsymbol{u}) + \boldsymbol{\lambda}_\tau - \boldsymbol{f} \\ \mathcal{R}_\nu^{\boldsymbol{\lambda}}(\boldsymbol{u}, \boldsymbol{\lambda}) = \boldsymbol{0} \\ \mathcal{R}_\tau^{\boldsymbol{\lambda}}(\dot{\boldsymbol{u}}_{\tau,p}, \boldsymbol{\lambda}_{\tau,p}) = \max(S, \|\boldsymbol{\lambda}_{\tau,p} + c_\tau\dot{\boldsymbol{u}}_{\tau,p}\|)\boldsymbol{\lambda}_{\tau,p} - S(\boldsymbol{\lambda}_{\tau,p} + c_\tau\dot{\boldsymbol{u}}_{\tau,p}) \end{pmatrix} = \boldsymbol{0}.$$

It leads to the following algorithm of index k

(i) Choose $(\boldsymbol{u}^{(0)}, \boldsymbol{\lambda}^{(0)})$, set $k = 0$.

(ii) Set $\mathcal{A}_\tau^{k+1} = \{p \in \mathcal{S} : \|\boldsymbol{\lambda}_{\tau,p}^{(k)} + c_\tau\dot{\boldsymbol{u}}_{\tau,p}^{(k)}\| > S\}$, $\mathcal{I}_\tau^{k+1} = \mathcal{S} \setminus \mathcal{A}_\tau^{k+1}$.

(iii) Find $(\boldsymbol{u}^{(k+1)}, \boldsymbol{\lambda}^{(k+1)})$ such that

$$\begin{aligned} &\rho\ddot{\boldsymbol{u}}^{(k+1)} + A(\boldsymbol{u}^{(k+1)}) + \boldsymbol{\lambda}_\tau^{(k+1)} = \boldsymbol{f}, \\ &u_{\nu,p}^{(k+1)} = 0 \quad \text{for all} \quad p \in \mathcal{S}, \\ &\dot{\boldsymbol{u}}_{\tau,p}^{(k+1)} = 0 \quad \text{for all} \quad p \in \mathcal{I}_\tau^{k+1}, \\ &\boldsymbol{L}_p^{(k)}\dot{\boldsymbol{u}}_{\tau,p}^{(k+1)} + \boldsymbol{\lambda}_{\tau,p}^{(k+1)} = \boldsymbol{r}_p^{(k)} \quad \text{for all} \quad p \in \mathcal{A}_\tau^{k+1}. \end{aligned} \tag{5.24}$$

(iv) If $\|(\boldsymbol{u}^{(k+1)}, \boldsymbol{\lambda}^{(k+1)}) - (\boldsymbol{u}^{(k)}, \boldsymbol{\lambda}^{(k)})\| \le \epsilon$, $\|\mathcal{R}(\boldsymbol{u}^{(k+1)}, \boldsymbol{\lambda}^{(k+1)})\| \le \epsilon$ and $\mathcal{A}_\tau^{k+1} = \mathcal{A}_\tau^k$ then stop, else goto (ii).

Remark. The nonlinear system (5.24) corresponding to $\mathcal{R}^{\boldsymbol{u}}(\boldsymbol{u}^{(k+1)}, \boldsymbol{\lambda}^{(k+1)}) = \boldsymbol{0}$ has to be solved by a Newton method at each active set iteration.

2D case

In this specific problem, and for a two dimensional case, one can obtain a simplified equivalent version of the algorithm. Let $\mathcal{G}_{\mathcal{R}_\tau^{\boldsymbol{\lambda}}}^{slip}$ be the generalized derivative of $\mathcal{R}_\tau^{\boldsymbol{\lambda}}$ in the slip case

$$\begin{aligned} \mathcal{G}_{\mathcal{R}_\tau^{\boldsymbol{\lambda}}}^{slip}(\dot{\boldsymbol{u}}_{\tau,p}, \boldsymbol{\lambda}_{\tau,p})(\delta\dot{\boldsymbol{u}}_{\tau,p}, \delta\boldsymbol{\lambda}_{\tau,p}) &= \boldsymbol{\lambda}_{\tau,p}\frac{(\boldsymbol{\lambda}_{\tau,p} + c_\tau\dot{\boldsymbol{u}}_{\tau,p})^T}{\|\boldsymbol{\lambda}_{\tau,p} + c_\tau\dot{\boldsymbol{u}}_{\tau,p}\|}(\delta\boldsymbol{\lambda}_{\tau,p} + c_\tau\delta\dot{\boldsymbol{u}}_{\tau,p}) \\ &- S(\delta\boldsymbol{\lambda}_{\tau,p} + c_\tau\delta\dot{\boldsymbol{u}}_{\tau,p}) + \|\boldsymbol{\lambda}_{\tau,p} + c_\tau\dot{\boldsymbol{u}}_{\tau,p}\|\delta\boldsymbol{\lambda}_{\tau,p}. \end{aligned} \tag{5.25}$$

Denote by τ, the unit slip vector; since the problem is bilateral, we have on the contact boundary

$$\boldsymbol{\lambda}_{\tau,p} = S\tau, \tag{5.26}$$

$$\frac{(\boldsymbol{\lambda}_{\tau,p} + c_\tau\dot{\boldsymbol{u}}_{\tau,p})}{\|\boldsymbol{\lambda}_{\tau,p} + c_\tau\dot{\boldsymbol{u}}_{\tau,p}\|} = \tau, \tag{5.27}$$

$$\delta\boldsymbol{\lambda}_{\tau,p} + c_\tau\delta\dot{\boldsymbol{u}}_{\tau,p} = \alpha\tau. \tag{5.28}$$

Combining (5.25)–(5.28), we get

$$\mathcal{G}_{\mathcal{R}_\tau^{\boldsymbol{\lambda}}}^{slip}(\dot{\boldsymbol{u}}_{\tau,p}, \boldsymbol{\lambda}_{\tau,p})(\delta\dot{\boldsymbol{u}}_{\tau,p}, \delta\boldsymbol{\lambda}_{\tau,p}) = S\alpha(\tau\tau^T - I_2)\tau + \|\boldsymbol{\lambda}_{\tau,p} + c_\tau\dot{\boldsymbol{u}}_{\tau,p}\|\delta\boldsymbol{\lambda}_{\tau,p}.$$

Since $\tau\tau^T + \nu\nu^T = I_2$ in the 2D case, we have:

$$(\tau\tau^T - I_2)\tau = \nu\nu^T\tau = \begin{pmatrix} 0 \\ 0 \end{pmatrix}.$$

Therefore, (5.23) becomes

$$\boldsymbol{\lambda}_{\tau,p}^{(k+1)} = S\frac{\boldsymbol{\lambda}_{\tau,p}^{(k)} + c_\tau\dot{\boldsymbol{u}}_{\tau,p}^{(k)}}{\|\boldsymbol{\lambda}_{\tau,p}^{(k)} + c_\tau\dot{\boldsymbol{u}}_{\tau,p}^{(k)}\|} = S\tau^{(k)} = \boldsymbol{\lambda}_{\tau,p}^{(k)}.$$

The simplified algorithm takes the following form
(i) Choose $(\boldsymbol{u}^{(0)}, \lambda^{(0)})$, set $k = 0$.
(ii) Set $\mathcal{A}_\tau^{k+1} = \{p \in \mathcal{S} : \|\boldsymbol{\lambda}_{\tau,p}^{(k)} + c_\tau \dot{\boldsymbol{u}}_{\tau,p}^{(k)}\| > S\}$, $\mathcal{I}_\tau^{k+1} = \mathcal{S} \setminus \mathcal{A}_\tau^{k+1}$.
(iii) Find $(\boldsymbol{u}^{(k+1)}, \lambda^{(k+1)})$ such that

$$\begin{aligned}
&\rho \ddot{\boldsymbol{u}}^{(k+1)} + A(\boldsymbol{u}^{(k+1)}) + \boldsymbol{\lambda}_\tau^{(k+1)} = \boldsymbol{f},\\
&u_{\nu,p}^{(k+1)} = 0 \quad \text{for all} \quad p \in \mathcal{S},\\
&\dot{\boldsymbol{u}}_{\tau,p}^{(k+1)} = 0 \quad \text{for all} \quad p \in \mathcal{I}_\tau^{k+1},\\
&\boldsymbol{\lambda}_{\tau,p}^{(k+1)} = S\frac{\boldsymbol{\lambda}_{\tau,p}^{(k)} + c_\tau \dot{\boldsymbol{u}}_{\tau,p}^{(k)}}{\|\boldsymbol{\lambda}_{\tau,p}^{(k)} + c_\tau \dot{\boldsymbol{u}}_{\tau,p}^{(k)}\|} \quad \text{for all} \quad p \in \mathcal{A}_\tau^{k+1}.
\end{aligned}$$

(iv) If $\|(\boldsymbol{u}^{(k+1)}, \lambda^{(k+1)}) - (\boldsymbol{u}^{(k)}, \lambda^{(k)})\| \le \epsilon$, $\|\mathcal{R}(\boldsymbol{u}^{(k+1)}, \lambda^{(k+1)})\| \le \epsilon$ and $\mathcal{A}_\tau^{k+1} = \mathcal{A}_\tau^k$ then stop, else goto (ii).

6. Coulomb's friction law with a gap

We consider now an unilateral contact with Coulomb's law of dry friction instead. Denoting by p the index of the vertices on $\Gamma_3^h \in \Gamma_3$ and with these considerations, the discrete conditions on the contact boundary are

$$u_{\nu,p} \le g, \tag{6.1}$$

$$\lambda_{\nu,p} \ge 0, \tag{6.2}$$

$$(u_{\nu,p} - g)\lambda_{\nu,p} = 0, \tag{6.3}$$

$$\begin{cases}
\|\boldsymbol{\lambda}_{\tau,p}\| \le \mu|\lambda_{\nu,p}|,\\
\|\boldsymbol{\lambda}_{\tau,p}\| < \mu|\lambda_{\nu,p}| \Longrightarrow \dot{\boldsymbol{u}}_{\tau,p} = 0,\\
\|\boldsymbol{\lambda}_{\tau,p}\| = \mu|\lambda_{\nu,p}| \Longrightarrow \exists \beta \ge 0 : \boldsymbol{\lambda}_{\tau,p} = \beta \dot{\boldsymbol{u}}_{\tau,p},
\end{cases} \tag{6.4}$$

The discrete Signorini conditions (6.1)–(6.3) are represented by the following nonlinear complementary function $\mathcal{R}_\nu^\lambda(u_{\nu,p}, \lambda_{\nu,p}) = 0$

$$\mathcal{R}_\nu^\lambda(u_{\nu,p}, \lambda_{\nu,p}) = \lambda_{\nu,p} - \max(0, \lambda_{\nu,p} + c_\nu(u_{\nu,p} - g)). \tag{6.5}$$

Such a result was already proved in [26]. In order to introduce the second nonlinear complementary function associated to the frictional conditions, that is to say equivalent to (6.4), one may consider (5.3) where $\mu\lambda_{\nu,p}$ is used instead of the Tresca's friction threshold S:

$$\mathcal{R}_\tau^\lambda(u_{\nu,p}, \dot{\boldsymbol{u}}_{\tau,p}, \lambda_{\nu,p}, \boldsymbol{\lambda}_{\tau,p}) = \max(\mu\lambda_{\nu,p}, \|\boldsymbol{\lambda}_{\tau,p} + c_\tau \dot{\boldsymbol{u}}_{\tau,p}\|)\boldsymbol{\lambda}_{\tau,p} - \mu\lambda_{\nu,p}(\boldsymbol{\lambda}_{\tau,p} + c_\tau \dot{\boldsymbol{u}}_{\tau,p}). \tag{6.6}$$

The proof of this result is quite similar to the one provided in the previous part. Now, we provide the generalized derivative of the complementary functions in the gap, stick and slip cases.

Gap case: $\lambda_{\nu,p} + c_\nu(u_{\nu,p} - g) \le 0$

$$\begin{aligned}
&\mathcal{R}_\nu^\lambda(u_{\nu,p}, \lambda_{\nu,p}) = \lambda_{\nu,p},\\
&\mathcal{R}_\tau^\lambda(u_{\nu,p}, \dot{\boldsymbol{u}}_{\tau,p}, \lambda_{\nu,p}, \boldsymbol{\lambda}_{\tau,p}) = \|\boldsymbol{\lambda}_{\tau,p} + c_\tau \dot{\boldsymbol{u}}_{\tau,p}\|\boldsymbol{\lambda}_{\tau,p}.
\end{aligned}$$

Then, since $\mathcal{R}_\tau^\lambda(u_{\nu,p}, \dot{\boldsymbol{u}}_{\tau,p}, \lambda_{\nu,p}, \boldsymbol{\lambda}_{\tau,p}) = 0$

$$d_{u_{\nu,p}}\mathcal{R}_\nu^\lambda = 0, \tag{6.7}$$

$$d_{\lambda_{\nu,p}}\mathcal{R}_\nu^\lambda = d\lambda_{\nu,p}, \tag{6.8}$$

$$d_{u_{\nu,p}}\mathcal{R}_\tau^\lambda = 0, \tag{6.9}$$

$$d_{\dot{\boldsymbol{u}}_{\tau,p}}\mathcal{R}_\tau^\lambda = c_\tau \boldsymbol{\lambda}_{\tau,p}\frac{(\boldsymbol{\lambda}_{\tau,p} + c_\tau \dot{\boldsymbol{u}}_{\tau,p})^T}{\|\boldsymbol{\lambda}_{\tau,p} + c_\tau \dot{\boldsymbol{u}}_{\tau,p}\|} d\dot{\boldsymbol{u}}_{\tau,p} = 0, \tag{6.10}$$

$$d_{\lambda_{\nu,p}}\mathcal{R}_\tau^\lambda = 0, \tag{6.11}$$

$$d_{\boldsymbol{\lambda}_{\tau,p}}\mathcal{R}_\tau^\lambda = \left(\boldsymbol{\lambda}_{\tau,p}\frac{(\boldsymbol{\lambda}_{\tau,p} + c_\tau \dot{\boldsymbol{u}}_{\tau,p})^T}{\|\boldsymbol{\lambda}_{\tau,p} + c_\tau \dot{\boldsymbol{u}}_{\tau,p}\|} + \|\boldsymbol{\lambda}_{\tau,p} + c_\tau \dot{\boldsymbol{u}}_{\tau,p}\|\boldsymbol{I}_2\right) d\boldsymbol{\lambda}_{\tau,p} \tag{6.12}$$

Stick case: $\mu\lambda_{\nu,p} \ge \|\boldsymbol{\lambda}_{\tau,p} + c_\tau \dot{\boldsymbol{u}}_{\tau,p}\| \ge 0$

$$\begin{aligned}
&\mathcal{R}_\nu^\lambda(u_{\nu,p}, \lambda_{\nu,p}) = -c_\nu(u_{\nu,p} - g),\\
&\mathcal{R}_\tau^\lambda(u_{\nu,p}, \dot{\boldsymbol{u}}_{\tau,p}, \lambda_{\nu,p}, \boldsymbol{\lambda}_{\tau,p}) = -\mu c_\tau \lambda_{\nu,p} \dot{\boldsymbol{u}}_{\tau,p}.
\end{aligned}$$

Then

$$d_{u_{\nu,p}}\mathcal{R}_{\nu}^{\lambda} = -c_{\nu}du_{\nu,p}, \tag{6.13}$$
$$d_{\lambda_{\nu,p}}\mathcal{R}_{\nu}^{\lambda} = 0, \tag{6.14}$$
$$d_{u_{\nu,p}}\mathcal{R}_{\tau}^{\lambda} = 0, \tag{6.15}$$
$$d_{\dot{\boldsymbol{u}}_{\tau,p}}\mathcal{R}_{\tau}^{\lambda} = -\mu c_{\tau}\lambda_{\nu,p}d\dot{\boldsymbol{u}}_{\tau,p}, \tag{6.16}$$
$$d_{\lambda_{\nu,p}}\mathcal{R}_{\tau}^{\lambda} = -\mu c_{\tau}\dot{\boldsymbol{u}}_{\tau,p}d\lambda_{\nu,p}, \tag{6.17}$$
$$d_{\boldsymbol{\lambda}_{\tau,p}}\mathcal{R}_{\tau}^{\lambda} = 0. \tag{6.18}$$

Slip case: $\|\boldsymbol{\lambda}_{\tau,p} + c_{\tau}\dot{\boldsymbol{u}}_{\tau,p}\| > \mu\lambda_{\nu,p} > 0$

$$\mathcal{R}_{\nu}^{\lambda}(u_{\nu,p}, \lambda_{\nu,p}) = -c_{\nu}(u_{\nu,p} - g),$$
$$\mathcal{R}_{\tau}^{\lambda}(u_{\nu,p}, \dot{\boldsymbol{u}}_{\tau,p}, \lambda_{\nu,p}, \boldsymbol{\lambda}_{\tau,p}) = \|\boldsymbol{\lambda}_{\tau,p} + c_{\tau}\dot{\boldsymbol{u}}_{\tau,p}\|\boldsymbol{\lambda}_{\tau,p} - \mu\lambda_{\nu,p}(\boldsymbol{\lambda}_{\tau,p} + c_{\tau}\dot{\boldsymbol{u}}_{\tau,p}).$$

Then

$$d_{u_{\nu,p}}\mathcal{R}_{\nu}^{\lambda} = -c_{\nu}du_{\nu,p}, \tag{6.19}$$
$$d_{\lambda_{\nu,p}}\mathcal{R}_{\nu}^{\lambda} = 0, \tag{6.20}$$
$$d_{u_{\nu,p}}\mathcal{R}_{\tau}^{\lambda} = 0, \tag{6.21}$$
$$d_{\dot{\boldsymbol{u}}_{\tau,p}}\mathcal{R}_{\tau}^{\lambda} = \Big(c_{\tau}\boldsymbol{\lambda}_{\tau,p}\frac{(\boldsymbol{\lambda}_{\tau,p} + c_{\tau}\dot{\boldsymbol{u}}_{\tau,p})^{T}}{\|\boldsymbol{\lambda}_{\tau,p} + c_{\tau}\dot{\boldsymbol{u}}_{\tau,p}\|} - \mu c_{\tau}\lambda_{\nu,p}\boldsymbol{I}_2\Big)d\dot{\boldsymbol{u}}_{\tau,p}, \tag{6.22}$$
$$d_{\lambda_{\nu,p}}\mathcal{R}_{\tau}^{\lambda} = -\mu(\boldsymbol{\lambda}_{\tau,p} + c_{\tau}\dot{\boldsymbol{u}}_{\tau,p})d\lambda_{\nu,p}, \tag{6.23}$$
$$d_{\boldsymbol{\lambda}_{\tau,p}}\mathcal{R}_{\tau}^{\lambda} = \Big(\boldsymbol{\lambda}_{\tau,p}\frac{(\boldsymbol{\lambda}_{\tau,p} + c_{\tau}\dot{\boldsymbol{u}}_{\tau,p})^{T}}{\|\boldsymbol{\lambda}_{\tau,p} + c_{\tau}\dot{\boldsymbol{u}}_{\tau,p}\|} + \|\boldsymbol{\lambda}_{\tau,p} + c_{\tau}\dot{\boldsymbol{u}}_{\tau,p}\|\boldsymbol{I}_2 - \mu\lambda_{\nu,p}\boldsymbol{I}_2\Big)d\boldsymbol{\lambda}_{\tau,p}. \tag{6.24}$$

By combining (6.7)–(6.24), with $\mathcal{G}_{\mathcal{R}_{\nu}^{\lambda}}$ and $\mathcal{G}_{\mathcal{R}_{\tau}^{\lambda}}$ the generalized derivative of $\mathcal{R}_{\nu}^{\lambda}$ and $\mathcal{R}_{\tau}^{\lambda}$, respectively, we obtain

$$\mathcal{G}_{\mathcal{R}_{\nu}^{\lambda}}(u_{\nu,p}, \lambda_{\nu,p})(\delta u_{\nu,p}, \delta\lambda_{\nu,p}) = -c_{\nu}(\mathcal{X}_{Stick} + \mathcal{X}_{Slip})\delta u_{\nu,p} + \mathcal{X}_{Gap}\delta\lambda_{\nu,p}, \tag{6.25}$$
$$\begin{aligned}\mathcal{G}_{\mathcal{R}_{\tau}^{\lambda}}(u_{\nu,p}, \dot{\boldsymbol{u}}_{\tau,p}, \lambda_{\nu,p}, \boldsymbol{\lambda}_{\tau,p})(\delta u_{\nu,p}, \delta\dot{\boldsymbol{u}}_{\tau,p}, \delta\lambda_{\nu,p}, \delta\boldsymbol{\lambda}_{\tau,p}) &= \mathcal{X}_{Gap}\|\boldsymbol{\lambda}_{\tau,p} + c_{\tau}\dot{\boldsymbol{u}}_{\tau,p}\|\delta\boldsymbol{\lambda}_{\tau,p} \\ &+ \mathcal{X}_{Stick}\Big(-\mu c_{\tau}\lambda_{\nu,p}\delta\dot{\boldsymbol{u}}_{\tau,p} - \mu c_{\tau}\dot{\boldsymbol{u}}_{\tau,p}\delta\lambda_{\nu,p}\Big) \\ &+ \mathcal{X}_{Slip}\Big(\Big(c_{\tau}\boldsymbol{\lambda}_{\tau,p}\frac{(\boldsymbol{\lambda}_{\tau,p} + c_{\tau}\dot{\boldsymbol{u}}_{\tau,p})^{T}}{\|\boldsymbol{\lambda}_{\tau,p} + c_{\tau}\dot{\boldsymbol{u}}_{\tau,p}\|} - \mu c_{\tau}\lambda_{\nu,p}\boldsymbol{I}_2\Big)\delta\dot{\boldsymbol{u}}_{\tau,p} - \mu(\boldsymbol{\lambda}_{\tau,p} + c_{\tau}\dot{\boldsymbol{u}}_{\tau,p})\delta\lambda_{\nu,p} \\ &+ \Big(\boldsymbol{\lambda}_{\tau,p}\frac{(\boldsymbol{\lambda}_{\tau,p} + c_{\tau}\dot{\boldsymbol{u}}_{\tau,p})^{T}}{\|\boldsymbol{\lambda}_{\tau,p} + c_{\tau}\dot{\boldsymbol{u}}_{\tau,p}\|} + \|\boldsymbol{\lambda}_{\tau,p} + c_{\tau}\dot{\boldsymbol{u}}_{\tau,p}\|\boldsymbol{I}_2 - \mu\lambda_{\nu,p}\boldsymbol{I}_2\Big)\delta\boldsymbol{\lambda}_{\tau,p}\Big)\end{aligned} \tag{6.26}$$

where

$$\mathcal{X}_{Gap} = 1, \mathcal{X}_{Stick} = 0, \mathcal{X}_{Slip} = 0 \text{ if } \lambda_{\nu,p} + c_{\nu}(u_{\nu,p} - g) \le 0,$$
$$\mathcal{X}_{Gap} = 0, \mathcal{X}_{Stick} = 1, \mathcal{X}_{Slip} = 0 \text{ if } \mu\lambda_{\nu,p} \ge \|\boldsymbol{\lambda}_{\tau,p} + c_{\tau}\dot{\boldsymbol{u}}_{\tau,p}\| > 0,$$
$$\mathcal{X}_{Gap} = 0, \mathcal{X}_{Stick} = 0, \mathcal{X}_{Slip} = 1 \text{ if } \|\boldsymbol{\lambda}_{\tau,p} + c_{\tau}\dot{\boldsymbol{u}}_{\tau,p}\| > \mu\lambda_{\nu,p} > 0.$$

Using now the semismooth Newton formalism at the current $(u_{\nu,p}^{(k)}, \dot{\boldsymbol{u}}_{\tau,p}^{(k)}, \lambda_{\nu,p}^{(k)}, \boldsymbol{\lambda}_{\tau,p}^{(k)})$, one can derive the new iterate $(u_{\nu,p}^{(k+1)}, \dot{\boldsymbol{u}}_{\tau,p}^{(k+1)}, \lambda_{\nu,p}^{(k+1)}, \boldsymbol{\lambda}_{\tau,p}^{(k+1)})$

$$\mathcal{G}_{\mathcal{R}_{\nu}^{\lambda}}(u_{\nu,p}^{(k)}, \lambda_{\nu,p}^{(k)})(\delta u_{\nu,p}^{(k+1)}, \delta\lambda_{\nu,p}^{(k+1)}) = -\mathcal{R}_{\nu}^{\lambda}(u_{\nu,p}^{(k)}, \lambda_{\nu,p}^{(k)}), \tag{6.27}$$
$$\begin{aligned}&\mathcal{G}_{\mathcal{R}_{\tau}^{\lambda}}(u_{\nu,p}^{(k)}, \dot{\boldsymbol{u}}_{\tau,p}^{(k)}, \lambda_{\nu,p}^{(k)}, \boldsymbol{\lambda}_{\tau,p}^{(k)})(\delta u_{\nu,p}^{(k+1)}, \delta\dot{\boldsymbol{u}}_{\tau,p}^{(k+1)}, \delta\lambda_{\nu,p}^{(k+1)}, \delta\boldsymbol{\lambda}_{\tau,p}^{(k+1)}) \\ &= -\mathcal{R}_{\tau}^{\lambda}(u_{\nu,p}^{(k)}, \dot{\boldsymbol{u}}_{\tau,p}^{(k)}, \lambda_{\nu,p}^{(k)}, \boldsymbol{\lambda}_{\tau,p}^{(k)}),\end{aligned} \tag{6.28}$$
$$\begin{aligned}&(u_{\nu,p}^{(k+1)}, \dot{\boldsymbol{u}}_{\tau,p}^{(k+1)}, \lambda_{\nu,p}^{(k+1)}, \boldsymbol{\lambda}_{\tau,p}^{(k+1)}) \\ &= (u_{\nu,p}^{(k)}, \dot{\boldsymbol{u}}_{\tau,p}^{(k)}, \lambda_{\nu,p}^{(k)}, \boldsymbol{\lambda}_{\tau,p}^{(k)}) + (\delta u_{\nu,p}^{(k+1)}, \delta\dot{\boldsymbol{u}}_{\tau,p}^{(k+1)}, \delta\lambda_{\nu,p}^{(k+1)}, \delta\boldsymbol{\lambda}_{\tau,p}^{(k+1)}).\end{aligned} \tag{6.29}$$

Gap case: $\mathcal{X}_{Gap} = 1, \mathcal{X}_{Stick} = 0, \mathcal{X}_{Slip} = 0$

$$\lambda_{\nu,p}^{(k+1)} - \lambda_{\nu,p}^{(k)} = -\lambda_{\nu,p}^{(k)}, \tag{6.30}$$
$$\|\boldsymbol{\lambda}_{\tau,p}^{(k)} + c_{\tau}\dot{\boldsymbol{u}}_{\tau,p}^{(k)}\|(\boldsymbol{\lambda}_{\tau,p}^{(k+1)} - \boldsymbol{\lambda}_{\tau,p}^{(k)}) = -\|\boldsymbol{\lambda}_{\tau,p}^{(k)} + c_{\tau}\dot{\boldsymbol{u}}_{\tau,p}^{(k)}\|\boldsymbol{\lambda}_{\tau,p}^{(k)}. \tag{6.31}$$

Next,

$$\lambda_{\nu,p}^{(k+1)} = 0, \tag{6.32}$$

$$\boldsymbol{\lambda}_{\tau,p}^{(k+1)} = 0, \tag{6.33}$$

since $\|\boldsymbol{\lambda}_{\tau,p}^{(k)} + c_\tau \dot{\boldsymbol{u}}_{\tau,p}^{(k)}\| > 0$.

Stick case: $\mathcal{X}_{Gap} = 0$, $\mathcal{X}_{Stick} = 1$, $\mathcal{X}_{Slip} = 0$

$$-c_\nu(u_{\nu,p}^{(k+1)} - u_{\nu,p}^{(k)}) = c_\nu(u_{\nu,p}^{(k)} - g), \tag{6.34}$$

$$-\mu c_\tau \lambda_{\nu,p}^{(k)}(\dot{\boldsymbol{u}}_{\tau,p}^{(k+1)} - \dot{\boldsymbol{u}}_{\tau,p}^{(k)}) - \mu c_\tau \dot{\boldsymbol{u}}_{\tau,p}^{(k)}(\lambda_{\nu,p}^{(k+1)} - \lambda_{\nu,p}^{(k)}) = \mu c_\tau \lambda_{\nu,p}^{(k)} \dot{\boldsymbol{u}}_{\tau,p}^{(k)}. \tag{6.35}$$

Next,

$$u_{\nu,p}^{(k+1)} = g, \tag{6.36}$$

$$\dot{\boldsymbol{u}}_{\tau,p}^{(k+1)} + \frac{\dot{\boldsymbol{u}}_{\tau,p}^{(k)}}{\lambda_{\nu,p}^{(k)}} \lambda_{\nu,p}^{(k+1)} = \dot{\boldsymbol{u}}_{\tau,p}^{(k)}. \tag{6.37}$$

Slip case: $\mathcal{X}_{Gap} = 0$, $\mathcal{X}_{Stick} = 0$, $\mathcal{X}_{Slip} = 1$

For $\mathcal{R}_\nu^\lambda$, we get once again

$$u_{\nu,p}^{(k+1)} = g. \tag{6.38}$$

For $\mathcal{R}_\tau^\lambda$, we obtain

$$\begin{aligned}
&\Big(c_\tau \lambda_{\tau,p}^{(k)} \frac{(\boldsymbol{\lambda}_{\tau,p}^{(k)} + c_\tau \dot{\boldsymbol{u}}_{\tau,p}^{(k)})^T}{\|\boldsymbol{\lambda}_{\tau,p}^{(k)} + c_\tau \dot{\boldsymbol{u}}_{\tau,p}^{(k)}\|} - \mu c_\tau \lambda_{\nu,p}^{(k)} \boldsymbol{I}_2\Big)(\dot{\boldsymbol{u}}_{\tau,p}^{(k+1)} - \dot{\boldsymbol{u}}_{\tau,p}^{(k)}) \\
&- \mu(\boldsymbol{\lambda}_{\tau,p}^{(k)} + c_\tau \dot{\boldsymbol{u}}_{\tau,p}^{(k)})(\lambda_{\nu,p}^{(k+1)} - \lambda_{\nu,p}^{(k)}) \\
&+ \Big(\boldsymbol{\lambda}_{\tau,p}^{(k)} \frac{(\boldsymbol{\lambda}_{\tau,p}^{(k)} + c_\tau \dot{\boldsymbol{u}}_{\tau,p}^{(k)})^T}{\|\boldsymbol{\lambda}_{\tau,p}^{(k)} + c_\tau \dot{\boldsymbol{u}}_{\tau,p}^{(k)}\|} + \|\boldsymbol{\lambda}_{\tau,p}^{(k)} + c_\tau \dot{\boldsymbol{u}}_{\tau,p}^{(k)}\| \boldsymbol{I}_2 - \mu \lambda_{\nu,p}^{(k)} \boldsymbol{I}_2\Big)(\boldsymbol{\lambda}_{\tau,p}^{(k+1)} - \boldsymbol{\lambda}_{\tau,p}^{(k)}) \\
&= -\|\boldsymbol{\lambda}_{\tau,p}^{(k)} + c_\tau \dot{\boldsymbol{u}}_{\tau,p}^{(k)}\| \boldsymbol{\lambda}_{\tau,p}^{(k)} + \mu \lambda_{\nu,p}^{(k)}(\boldsymbol{\lambda}_{\tau,p}^{(k)} + c_\tau \dot{\boldsymbol{u}}_{\tau,p}^{(k)}).
\end{aligned} \tag{6.39}$$

For recall,

$$\boldsymbol{F}^{(k)} = \boldsymbol{\lambda}_{\tau,p}^{(k)} \frac{(\boldsymbol{\lambda}_{\tau,p}^{(k)} + c_\tau \dot{\boldsymbol{u}}_{\tau,p}^{(k)})^T}{\|\boldsymbol{\lambda}_{\tau,p}^{(k)} + c_\tau \dot{\boldsymbol{u}}_{\tau,p}^{(k)}\|},$$

$$E^{(k)} = \frac{1}{\|\boldsymbol{\lambda}_{\tau,p}^{(k)} + c_\tau \dot{\boldsymbol{u}}_{\tau,p}^{(k)}\|}.$$

Therefore, after an elementary computation

$$\begin{aligned}
&c_\tau E^{(k)}\Big(\boldsymbol{F}^{(k)} - \mu \lambda_{\nu,p}^{(k)} \boldsymbol{I}_2\Big)(\dot{\boldsymbol{u}}_{\tau,p}^{(k+1)} - \dot{\boldsymbol{u}}_{\tau,p}^{(k)}) - \mu E^{(k)}(\boldsymbol{\lambda}_{\tau,p}^{(k)} + c_\tau \dot{\boldsymbol{u}}_{\tau,p}^{(k)}) \lambda_{\nu,p}^{(k+1)} \\
&+ \Big(E^{(k)}(\boldsymbol{F}^{(k)} - \mu \lambda_{\nu,p}^{(k)} \boldsymbol{I}_2) + \boldsymbol{I}_2\Big) \boldsymbol{\lambda}_{\tau,p}^{(k+1)} - E^{(k)}\Big(\boldsymbol{F}^{(k)} - \mu \lambda_{\nu,p}^{(k)} \boldsymbol{I}_2\Big) \boldsymbol{\lambda}_{\tau,p}^{(k)} = 0.
\end{aligned}$$

Now, let

$$\boldsymbol{M}_p^{*(k)} = E^{(k)}(\boldsymbol{F}^{(k)} - \mu \lambda_{\nu,p}^{(k)} \boldsymbol{I}_2),$$

$$\boldsymbol{h}_p^{(k)} = E^{(k)} \boldsymbol{F}^{(k)}\Big(\boldsymbol{\lambda}_{\tau,p}^{(k)} + c_\tau \dot{\boldsymbol{u}}_{\tau,p}^{(k)}\Big).$$

Then

$$\begin{aligned}
&c_\tau \boldsymbol{M}_p^{*(k)} \dot{\boldsymbol{u}}_{\tau,p}^{(k+1)} - \mu E^{(k)}(\boldsymbol{\lambda}_{\tau,p}^{(k)} + c_\tau \dot{\boldsymbol{u}}_{\tau,p}^{(k)}) \lambda_{\nu,p}^{(k+1)} + \Big(\boldsymbol{I}_2 + \boldsymbol{M}_p^{*(k)}\Big) \boldsymbol{\lambda}_{\tau,p}^{(k+1)} \\
&= \boldsymbol{h}_p^{(k)} - \mu E^{(k)}(\boldsymbol{\lambda}_{\tau,p}^{(k)} + c_\tau \dot{\boldsymbol{u}}_{\tau,p}^{(k)}) \lambda_{\nu,p}^{(k)}.
\end{aligned}$$

In order to simplify even further the notations, we introduce the following operators:

$$\boldsymbol{L}_p^{*(k)} = c_\tau(\boldsymbol{I}_2 + \boldsymbol{M}_p^{*(k)})^{-1} \boldsymbol{M}_p^{*(k)},$$

$$\boldsymbol{r}_p^{*(k)} = (\boldsymbol{I}_2 + \boldsymbol{M}_p^{*(k)})^{-1} \boldsymbol{h}_p^{(k)},$$

$$\boldsymbol{v}_p^{(k)} = \mu(\boldsymbol{I}_2 + \boldsymbol{M}_p^{*(k)})^{-1} E^{(k)}(\boldsymbol{\lambda}_{\tau,p}^{(k)} + c_\tau \dot{\boldsymbol{u}}_{\tau,p}^{(k)}).$$

And, at last

$$\boldsymbol{L}_p^{*(k)}\dot{\boldsymbol{u}}_{\tau,p}^{(k+1)} - \boldsymbol{v}_p^{(k)}\lambda_{\nu,p}^{(k+1)} + \boldsymbol{\lambda}_{\tau,p}^{(k+1)} = \boldsymbol{r}_p^{*(k)} - \boldsymbol{v}_p^{(k)}\lambda_{\nu,p}^{(k)}.$$

2D case

Gap case: $\mathcal{X}_{Gap} = 1$, $\mathcal{X}_{Stick} = 0$, $\mathcal{X}_{Slip} = 0$

$$\lambda_{\nu,p}^{(k+1)} = 0, \tag{6.40}$$

$$\boldsymbol{\lambda}_{\tau,p}^{(k+1)} = 0, \tag{6.41}$$

Stick case: $\mathcal{X}_{Gap} = 0$, $\mathcal{X}_{Stick} = 1$, $\mathcal{X}_{Slip} = 0$

$$u_{\nu,p}^{(k+1)} = g, \tag{6.42}$$

$$\dot{\boldsymbol{u}}_{\tau,p}^{(k+1)} + \frac{\dot{\boldsymbol{u}}_{\tau,p}^{(k)}}{\lambda_{\nu,p}^{(k)}}\lambda_{\nu,p}^{(k+1)} = \dot{\boldsymbol{u}}_{\tau,p}^{(k)}. \tag{6.43}$$

Slip case: $\mathcal{X}_{Gap} = 0$, $\mathcal{X}_{Stick} = 0$, $\mathcal{X}_{Slip} = 1$

$$u_{\nu,p}^{(k+1)} = g. \tag{6.44}$$

By using (5.26)–(5.28) and $\tau\tau^T + \nu\nu^T = I_2$, we deduce from (6.39) the following expression

$$\begin{aligned} &-\mu(\boldsymbol{\lambda}_{\tau,p}^{(k)} + c_\tau\dot{\boldsymbol{u}}_{\tau,p}^{(k)})(\lambda_{\nu,p}^{(k+1)} - \lambda_{\nu,p}^{(k)}) + \|\boldsymbol{\lambda}_{\tau,p}^{(k)} + c_\tau\dot{\boldsymbol{u}}_{\tau,p}^{(k)}\|(\lambda_{\tau,p}^{(k+1)} - \lambda_{\tau,p}^{(k)}) \\ &= -\|\boldsymbol{\lambda}_{\tau,p}^{(k)} + c_\tau\dot{\boldsymbol{u}}_{\tau,p}^{(k)}\|\boldsymbol{\lambda}_{\tau,p}^{(k)} + \mu\lambda_{\nu,p}^{(k)}(\boldsymbol{\lambda}_{\tau,p}^{(k)} + c_\tau\dot{\boldsymbol{u}}_{\tau,p}^{(k)}). \end{aligned} \tag{6.45}$$

Therefore, after an elementary computation

$$\boldsymbol{\lambda}_{\tau,p}^{(k+1)} = \mu\lambda_{\nu,p}^{(k+1)}\frac{(\boldsymbol{\lambda}_{\tau,p}^{(k)} + c_\tau\dot{\boldsymbol{u}}_{\tau,p}^{(k)})}{\|\boldsymbol{\lambda}_{\tau,p}^{(k)} + c_\tau\dot{\boldsymbol{u}}_{\tau,p}^{(k)}\|} = \mu\lambda_{\nu,p}^{(k+1)}\tau^{(k)}.$$

7. Full iterative scheme for the Coulomb's friction law with a gap case

Let us denote by $\mathcal{S}$ the set of all nodes of the finite element mesh belonging to Γ_3^h and p the index of a node belonging to $\mathcal{S}$.

7.1. "Full" primal–dual active set

The discrete friction contact condition (6.1)–(6.4) are realized by applying an active set strategy on the nonlinear complementary functions $\mathcal{R}_\nu^\lambda$ and $\mathcal{R}_\tau^\lambda$ based on the Newton semi-smooth scheme derived in part 4. The active and inactive sets are defined as follows

$$\begin{aligned} \mathcal{A}_\nu^{k+1} &= \{p \in \mathcal{S} : \lambda_{\nu,p}^{(k)} + c_\nu(u_{\nu,p}^{(k)} - g) > 0\}, \\ \mathcal{I}_\nu^{k+1} &= \{p \in \mathcal{S} : \lambda_{\nu,p}^{(k)} + c_\nu(u_{\nu,p}^{(k)} - g) \le 0\}, \\ \mathcal{A}_\tau^{k+1} &= \{p \in \mathcal{S} : \|\boldsymbol{\lambda}_{\tau,p}^{(k)} + c_\tau\dot{\boldsymbol{u}}_{\tau,p}^{(k)}\| - \mu\lambda_{\nu,p}^{(k)} > 0\}, \\ \mathcal{I}_\tau^{k+1} &= \{p \in \mathcal{S} : \|\boldsymbol{\lambda}_{\tau,p}^{(k)} + c_\tau\dot{\boldsymbol{u}}_{\tau,p}^{(k)}\| - \mu\lambda_{\nu,p}^{(k)} \le 0\}. \end{aligned}$$

The status of a given node at the iteration k depends on the set it belongs to; based on the previous part it can be either in the non-contact, slip or stick status.

At each increment n for the time $t_{n-\frac{1}{2}}$, we also introduce $\mathcal{R}$ which describes the system of nonlinear equations arising from the discretized problem $\mathcal{P}_S^{nodal}$ in the case of unilateral contact and Coulomb friction, defined by

$$\mathcal{R}(\boldsymbol{u},\boldsymbol{\lambda}) = \begin{pmatrix} \mathcal{R}^{\boldsymbol{u}}(\boldsymbol{u},\boldsymbol{\lambda}) = \rho\ddot{\boldsymbol{u}} + A(\boldsymbol{u}) + \lambda_\nu\boldsymbol{\nu} + \boldsymbol{\lambda}_\tau - \boldsymbol{f} \\ \mathcal{R}_\nu^\lambda(\boldsymbol{u},\boldsymbol{\lambda}) = \lambda_{\nu,p} - \max(0, \lambda_{\nu,p} + c_\nu(u_{\nu,p} - g)) \\ \mathcal{R}_\tau^\lambda(\boldsymbol{u},\boldsymbol{\lambda}) = \max(\mu\lambda_{\nu,p}, \|\boldsymbol{\lambda}_{\tau,p} + c_\tau\dot{\boldsymbol{u}}_{\tau,p}\|)\boldsymbol{\lambda}_{\tau,p} - \mu\lambda_{\nu,p}(\boldsymbol{\lambda}_{\tau,p} + c_\tau\dot{\boldsymbol{u}}_{\tau,p}) \end{pmatrix} = \boldsymbol{0}.$$

Now, we turn to the description of the iterative active set algorithm of index k.

(i) Choose $(\boldsymbol{u}^{(0)}, \boldsymbol{\lambda}^{(0)})$, $c_\nu > 0$, $c_\tau > 0$ and set $k = 0$.

(ii) Set the active and inactive sets:

$$\begin{aligned} \mathcal{A}_\nu^{k+1} &= \{p \in \mathcal{S} : \lambda_{\nu,p}^{(k)} + c_\nu(u_{\nu,p}^{(k)} - g) > 0\}, \\ \mathcal{I}_\nu^{k+1} &= \mathcal{S} \setminus \mathcal{A}_\nu^{k+1}, \\ \mathcal{A}_\tau^{k+1} &= \{p \in \mathcal{S} : \|\boldsymbol{\lambda}_{\tau,p}^{(k)} + c_\tau\dot{\boldsymbol{u}}_{\tau,p}^{(k)}\| - \mu\lambda_{\nu,p}^{(k)} > 0\}, \\ \mathcal{I}_\tau^{k+1} &= \mathcal{S} \setminus \mathcal{A}_\tau^{k+1}. \end{aligned}$$

(iii) Find $(\boldsymbol{u}^{(k+1)}, \lambda^{(k+1)})$ such that

$$\rho\ddot{\boldsymbol{u}}^{(k+1)} + A(\boldsymbol{u}^{(k+1)}) + \lambda_{\nu}^{(k+1)}\nu + \boldsymbol{\lambda}_{\tau}^{(k+1)} = \boldsymbol{f}, \tag{7.1}$$

$$u_{\nu,p}^{(k+1)} = g \quad \text{for all} \quad p \in \mathcal{A}_{\nu}^{k+1}, \tag{7.2}$$

$$\lambda_{\nu,p}^{(k+1)} = 0, \quad \boldsymbol{\lambda}_{\tau,p}^{(k+1)} = 0 \quad \text{for all} \quad p \in \mathcal{I}_{\nu}^{k+1}, \tag{7.3}$$

$$\boldsymbol{L}_p^{*(k)}\dot{\boldsymbol{u}}_{\tau,p}^{(k+1)} - \boldsymbol{v}_p^{(k)}\lambda_{\nu,p}^{(k+1)} + \boldsymbol{\lambda}_{\tau,p}^{(k+1)} = \boldsymbol{r}_p^{*(k)} - \boldsymbol{v}_p^{(k)}\lambda_{\nu,p}^{(k)} \quad \text{for all } p \in \mathcal{A}_{\tau}^{k+1} \cap \mathcal{A}_{\nu}^{k+1}, \tag{7.4}$$

$$\dot{\boldsymbol{u}}_{\tau,p}^{(k+1)} + \frac{\dot{\boldsymbol{u}}_{\tau,p}^{(k)}}{\lambda_{\nu,p}^{(k)}}\lambda_{\nu,p}^{(k+1)} = \dot{\boldsymbol{u}}_{\tau,p}^{(k)} \quad \text{for all} \quad p \in \mathcal{I}_{\tau}^{k+1} \cap \mathcal{A}_{\nu}^{k+1}. \tag{7.5}$$

(iv) If $\|(\boldsymbol{u}^{(k+1)}, \lambda^{(k+1)}) - (\boldsymbol{u}^{(k)}, \lambda^{(k)})\| \leq \epsilon$, $\|\mathcal{R}(\boldsymbol{u}^{(k+1)}, \lambda^{(k+1)})\| \leq \epsilon$, $\mathcal{A}_{\nu}^{k+1} = \mathcal{A}_{\nu}^{k}$ and $\mathcal{A}_{\tau}^{k+1} = \mathcal{A}_{\tau}^{k}$ then stop, else goto (ii).

Remark. The nonlinear system (7.1) corresponding to $\mathcal{R}^{\boldsymbol{u}}(\boldsymbol{u}^{(k+1)}, \lambda^{(k+1)}) = \boldsymbol{0}$ has to be solved by a Newton method at each active set iteration.

2D case

For the 2D case, we turn to the following iterative active set algorithm of index k.
(i) Choose $(\boldsymbol{u}^{(0)}, \lambda^{(0)})$, $c_{\nu} > 0$, $c_{\tau} > 0$ and set $k = 0$.
(ii) Set the active and inactive sets:

$$\mathcal{A}_{\nu}^{k+1} = \{p \in \mathcal{S} : \lambda_{\nu,p}^{(k)} + c_{\nu}(u_{\nu,p}^{(k)} - g) > 0\},$$
$$\mathcal{I}_{\nu}^{k+1} = \mathcal{S} \setminus \mathcal{A}_{\nu}^{k+1},$$
$$\mathcal{A}_{\tau}^{k+1} = \{p \in \mathcal{S} : \|\boldsymbol{\lambda}_{\tau,p}^{(k)} + c_{\tau}\dot{\boldsymbol{u}}_{\tau,p}^{(k)}\| - \mu\lambda_{\nu,p}^{(k)} > 0\},$$
$$\mathcal{I}_{\tau}^{k+1} = \mathcal{S} \setminus \mathcal{A}_{\tau}^{k+1}.$$

(iii) Find $(\boldsymbol{u}^{(k+1)}, \lambda^{(k+1)})$ such that

$$\rho\ddot{\boldsymbol{u}}^{(k+1)} + A(\boldsymbol{u}^{(k+1)}) + \lambda_{\nu}^{(k+1)}\nu + \boldsymbol{\lambda}_{\tau}^{(k+1)} = \boldsymbol{f}, \tag{7.6}$$

$$u_{\nu,p}^{(k+1)} = g \quad \text{for all} \quad p \in \mathcal{A}_{\nu}^{k+1}, \tag{7.7}$$

$$\lambda_{\nu,p}^{(k+1)} = 0, \quad \boldsymbol{\lambda}_{\tau,p}^{(k+1)} = \boldsymbol{0} \quad \text{for all} \quad p \in \mathcal{I}_{\nu}^{k+1}, \tag{7.8}$$

$$\boldsymbol{\lambda}_{\tau,p}^{(k+1)} = \mu\lambda_{\nu,p}^{(k+1)}\frac{(\boldsymbol{\lambda}_{\tau,p}^{(k)} + c_{\tau}\dot{\boldsymbol{u}}_{\tau,p}^{(k)})}{\|\boldsymbol{\lambda}_{\tau,p}^{(k)} + c_{\tau}\dot{\boldsymbol{u}}_{\tau,p}^{(k)}\|} \quad \text{for all } p \in \mathcal{A}_{\tau}^{k+1} \cap \mathcal{A}_{\nu}^{k+1}, \tag{7.9}$$

$$\dot{\boldsymbol{u}}_{\tau,p}^{(k+1)} + \frac{\dot{\boldsymbol{u}}_{\tau,p}^{(k)}}{\lambda_{\nu,p}^{(k)}}\lambda_{\nu,p}^{(k+1)} = \dot{\boldsymbol{u}}_{\tau,p}^{(k)} \quad \text{for all} \quad p \in \mathcal{I}_{\tau}^{k+1} \cap \mathcal{A}_{\nu}^{k+1}. \tag{7.10}$$

(iv) If $\|(\boldsymbol{u}^{(k+1)}, \lambda^{(k+1)}) - (\boldsymbol{u}^{(k)}, \lambda^{(k)})\| \leq \epsilon$, $\|\mathcal{R}(\boldsymbol{u}^{(k+1)}, \lambda^{(k+1)})\| \leq \epsilon$, $\mathcal{A}_{\nu}^{k+1} = \mathcal{A}_{\nu}^{k}$ and $\mathcal{A}_{\tau}^{k+1} = \mathcal{A}_{\tau}^{k}$ then stop, else goto (ii).

7.2. "Inexact" primal–dual active set with fixed point method

In the case we consider a fixed point method related to the friction bound, we can approximate the Coulomb friction by a succession of states of Tresca friction in which the friction bound is fixed at each fixed point iteration of index i (cf [21]). Since we have notice that (7.10) can lead to numerical instabilities when $\lambda_{\nu,p}^{(k)}$ is small, we introduce a variant of the previous method. In this way, we have to introduce the couple $(\boldsymbol{u}^{(i,k)}, \lambda^{(i,k)})$ which represents the value of $(\boldsymbol{u}, \lambda)$ at the ith fixed point iteration and at the kth active set iteration. Moreover, $(\boldsymbol{u}^{(i-1,.)}, \lambda^{(i-1,.)})$ represents the value of $(\boldsymbol{u}, \lambda)$ obtained at the convergence of the active set method for the fixed point iteration $i-1$. Therefore, for each active set iteration, we fix the friction bound $\lambda_{\nu,p}^{(i,k+1)}$ to the value $\lambda_{\nu,p}^{(i-1,.)}$ obtained at the previous fixed point iteration. Then, the condition (7.10) leads to $\dot{\boldsymbol{u}}_{\tau,p}^{(k+1)} = 0$.

For the 2D case, we can consider the following active set algorithm of index k coupled with a fixed point method of index i:
(i) Choose $(\boldsymbol{u}^{(0,.)}, \lambda^{(0,.)})$ and set $i = 1$.
(ii) Set $(\boldsymbol{u}^{(i,0)}, \lambda^{(i,0)}) = (\boldsymbol{u}^{(i-1,.)}, \lambda^{(i-1,.)})$, $c_{\nu} > 0$, $c_{\tau} > 0$ and set $k = 0$.
(iii) Set the active and inactive sets:

$$\mathcal{A}_{\nu}^{k+1} = \{p \in \mathcal{S} : \lambda_{\nu,p}^{(i,k)} + c_{\nu}(u_{\nu,p}^{(i,k)} - g) > 0\},$$
$$\mathcal{I}_{\nu}^{k+1} = \mathcal{S} \setminus \mathcal{A}_{\nu}^{k+1},$$
$$\mathcal{A}_{\tau}^{k+1} = \{p \in \mathcal{S} : \|\boldsymbol{\lambda}_{\tau,p}^{(i,k)} + c_{\tau}\dot{\boldsymbol{u}}_{\tau,p}^{(i,k)}\| - \mu\lambda_{\nu,p}^{(i,k)} > 0\},$$
$$\mathcal{I}_{\tau}^{k+1} = \mathcal{S} \setminus \mathcal{A}_{\tau}^{k+1}.$$

(iv) Find $(\boldsymbol{u}^{(i,k+1)}, \lambda^{(i,k+1)})$ such that

$$\rho\ddot{\boldsymbol{u}}^{(k+1)} + A(\boldsymbol{u}^{(i,k+1)}) + \lambda_{\nu}^{(i,k+1)}\nu + \boldsymbol{\lambda}_{\tau}^{(i,k+1)} = \boldsymbol{f}, \tag{7.11}$$

$$u_{\nu,p}^{(i,k+1)} = g \quad \text{for all} \quad p \in \mathcal{A}_{\nu}^{k+1}, \tag{7.12}$$

$$\lambda_{\nu,p}^{(i,k+1)} = 0, \quad \boldsymbol{\lambda}_{\tau,p}^{(i,k+1)} = \boldsymbol{0} \quad \text{for all} \quad p \in \mathcal{I}_{\nu}^{k+1}, \tag{7.13}$$

$$\boldsymbol{\lambda}_{\tau,p}^{(i,k+1)} = \mu\lambda_{\nu,p}^{(i-1,.)} \frac{(\boldsymbol{\lambda}_{\tau,p}^{(i,k)} + c_{\tau}\dot{\boldsymbol{u}}_{\tau,p}^{(i,k)})}{\|\boldsymbol{\lambda}_{\tau,p}^{(i,k)} + c_{\tau}\dot{\boldsymbol{u}}_{\tau,p}^{(i,k)}\|} \quad \text{for all } p \in \mathcal{A}_{\tau}^{k+1} \cap \mathcal{A}_{\nu}^{k+1}, \tag{7.14}$$

$$\dot{\boldsymbol{u}}_{\tau,p}^{(i,k+1)} = \boldsymbol{0} \quad \text{for all} \quad p \in \mathcal{I}_{\tau}^{k+1} \cap \mathcal{A}_{\nu}^{k+1}. \tag{7.15}$$

(v) If $\|(\boldsymbol{u}^{(i,k+1)}, \lambda^{(i,k+1)}) - (\boldsymbol{u}^{(i,k)}, \lambda^{(i,k)})\| \leq \epsilon$, $\|\mathcal{R}(\boldsymbol{u}^{(i,k+1)}, \lambda^{(i,k+1)})\| \leq \epsilon$, $\mathcal{A}_{\nu}^{k+1} = \mathcal{A}_{\nu}^{k}$ and $\mathcal{A}_{\tau}^{k+1} = \mathcal{A}_{\tau}^{k}$ then stop and set $(\boldsymbol{u}^{(i,.)}, \lambda^{(i,.)}) = (\boldsymbol{u}^{(i,k+1)}, \lambda^{(i,k+1)})$, else goto (iii) with $k = k + 1$.
(vi) If $\|(\boldsymbol{u}^{(i,.)}, \lambda^{(i,.)}) - (\boldsymbol{u}^{(i-1,.)}, \lambda^{(i-1,.)})\| \leq \epsilon$, $\|\mathcal{R}(\boldsymbol{u}^{(i,.)}, \lambda^{(i,.)})\| \leq \epsilon$, then stop, else goto (ii) with $i = i + 1$.

Before presenting our numerical results, we would like to point out an interesting feature of the Inexact Active Set method that we expect to demonstrate in the following sections. It turns out such a method has the particularity of having symmetric linearized systems, unlike the linearized systems resulting from the Augmented Quasi Lagrangian for the 2D friction problems. This feature makes it possible to counterbalance the well-known slowness of the fixed point. Despite this fact, the fixed point method is strongly dependent on the coefficient of friction, unlike the augmented Lagrangian method, we refer to [4] and [8] for more details on this subject.

The next two sections are devoted to the numerical results, first in the static case then in the dynamic case.

8. Numerical simulations in the static case

The aim of this section is to provide numerical simulations on academic static cases to depict the mechanical behavior of the contact problem's solution $\mathcal{P}$. We display numerical simulations based on two static configurations: the bilinear contact with Tresca's law of friction and the unilateral contact with Coulomb's law of friction, both for a linear elastic beam on a perfectly rigid foundation. The numerical solution of Problem $\mathcal{P}$ is computed both with the active set method, described in Sections 5–7, and the Augmented Lagrangian method in order to highlight the performances and accuracy of the former compared to the latter, since an analytical solution is not available. For the Augmented Lagrangian method (cf [1]), it is required to introduce in the initial mesh additional fictitious nodes corresponding to the Lagrange multipliers. Note that the way these nodes are taken into account depends on the contact element considered for the spacial discretization of the interface Γ_3. In this section, the discretization use a "node-to-rigid" type of contact element, that is to say a set composed of one node of the contact boundary Γ_3 and one additional Lagrange multiplier node. For more details on Computational Contact Mechanics, we refer to [1,9,12,37,38].

In this section, the domain Ω is the cross section of a three-dimensional deformable body submitted to the action of traction forces so that a plane deformation hypothesis can be assumed. The details of the physical setting are given as follows. The foundation is defined by $\{(x_1, x_2) \in \mathbb{R}^2 : x_2 \leq 0\}$ for the case of bilinear contact with Tresca's law (see Fig. 2), and by $\{(x_1, x_2) \in \mathbb{R}^2 : x_2 \leq -1\}$ for the case of unilateral contact (see Fig. 6). The domain is defined by

$$\begin{aligned}
\Omega &= \{(x_1, x_2) \in \mathbb{R}^2 : x_1 \in]0, 10[\ ; \ x_2 \in]0, 1[\}, \\
\Gamma_1 &= \{(x_1, x_2) \in \mathbb{R}^2 : x_1 = 0 \ ; \ x_2 \in [0, 1]\}, \\
\Gamma_2 &= \{(x_1, x_2) \in \mathbb{R}^2 : x_1 \in]0, 10[\ ; \ x_2 = 1\} \cup \{(x_1, x_2) \in \mathbb{R}^2 : x_1 = 10 \ ; \ x_2 \in [0, 1]\}, \\
\Gamma_3 &= \{(x_1, x_2) \in \mathbb{R}^2 : x_1 \in]0, 10[\ ; \ x_2 = 0\}.
\end{aligned}$$

The displacement field is constrained on Γ_1. The part of the boundary Γ_2 is subjected to vertical traction of density $\boldsymbol{f}_2$. The body lies on the part Γ_3 of its boundary, whose behavior at the interface is described by a friction contact law. Regarding the spatial discretization, the number of nodes on Γ_3 is parametrized by *nbc*. The behavior constitutive law of the material is described by an elastic linear law where the elasticity tensor, denoted by $\mathcal{E}$, satisfies the following equation

$$(\mathcal{E}\boldsymbol{\varepsilon})_{\alpha\beta} = \frac{E\kappa}{(1+\kappa)(1-2\kappa)}(\boldsymbol{\varepsilon}_{11} + \boldsymbol{\varepsilon}_{22})\delta_{\alpha\beta} + \frac{E}{1+\kappa}\boldsymbol{\varepsilon}_{\alpha\beta}, \qquad 1 \leq \alpha, \beta \leq 2,$$

with E, κ and $\delta_{\alpha\beta}$ be respectively the Young modulus, the Poisson ratio of the material and the Kronecker symbol.

8.1. Bilateral contact and Tresca friction example

For $nbc = 128$, as depicted in Fig. 2, 9728 2D elastic elements were considered for 10 024 degrees of freedom. The interaction between the foundation and the deformable body is depicted by a bilinear contact law with Tresca's law of friction.

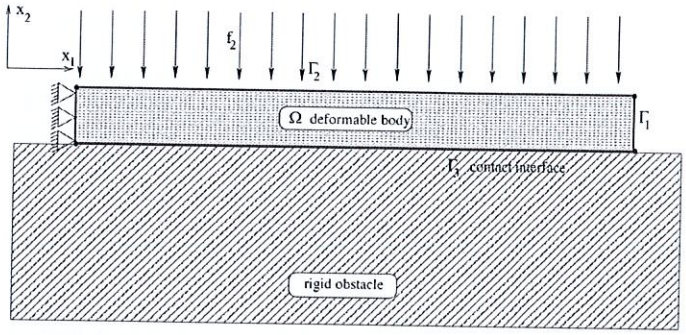

Fig. 2. Physical setting of the bilateral beam against a foundation.

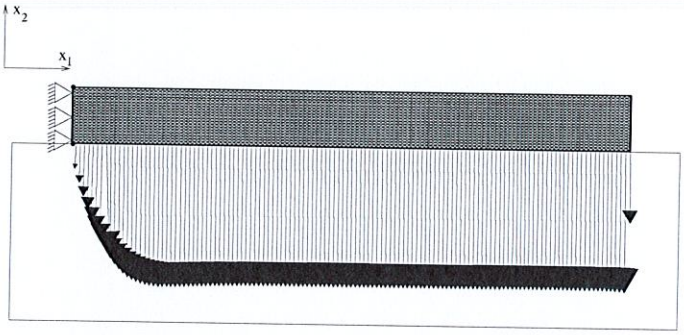

Fig. 3. Deformed configuration of the bilateral beam against a foundation.

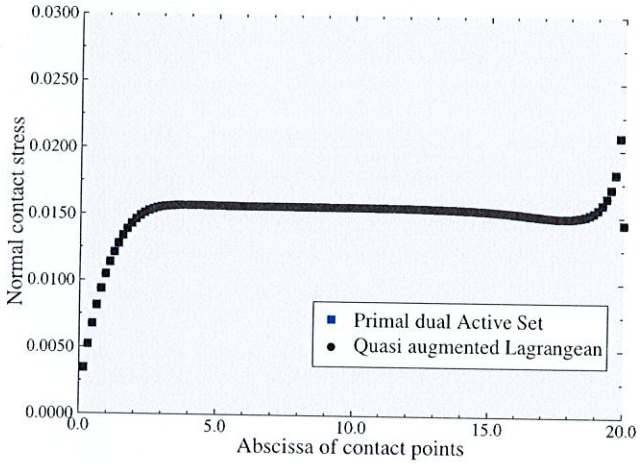

Fig. 4. Normal contact stresses on the contact area.

We provide below the value of the parameters used for the computation:

$E = 100\ \mathrm{N/m^2}, \quad \kappa = 0.3,$
$\boldsymbol{f}_0 = (0, 0)\ \mathrm{N/m^2}, \quad \boldsymbol{f}_2 = (0, -0.1)\,\mathrm{N/m} \quad \text{on } \Gamma_2,$
$c_\nu = 10, \quad c_\tau = 10, \quad r_{lagrangian} = 0.1$
stopping criterion : $\epsilon = 10^{-6}$.

In Fig. 3, we plot the deformed configuration and the frictional contact stresses on the boundary Γ_3.

Accuracy of the active set method comparing to the augmented Lagrangian method.

First, we investigate the accuracy of the active set method of the finite element model by comparing it to the well-known quasi-Augmented Lagrangian (cf [1]). The boundary Γ_3 is divided into 128 equal parts; the normal contact stress σ_ν and tangential friction stress $\|\sigma_\tau\|$ with respect to the abscissa is plotted in Figs. 4 and 5 for each method. We note that, for σ_ν and $\|\sigma_\tau\|$, there is no notable difference ($\approx 1.10^{-7}$), thus confirming the accuracy for this test case.

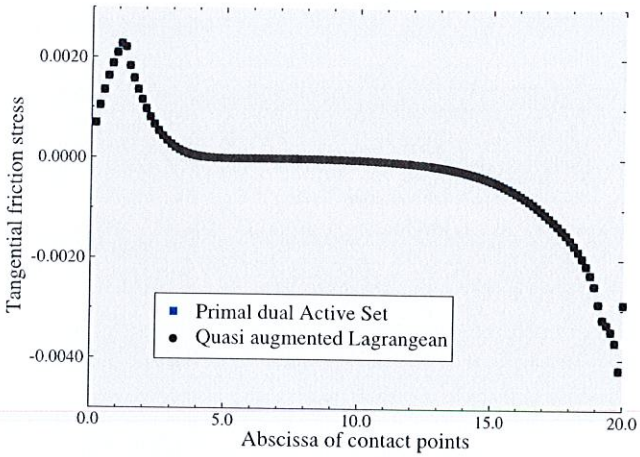

Fig. 5. Tangential friction stresses on the contact area.

Table 1
Results of the active set method for the bilateral contact and Tresca friction laws in comparison with the number of degrees of freedom (dof), the number of contact nodes (nbc), the Newton iterations (Nit) and the total CPU time (CPU) in seconds.

nbc	8	16	32	64	128	256	512
dof	76	166	586	2414	10024	40528	162976
Nit	7	9	9	11	12	13	13
CPU	<1	<1	<1	2	11	70	454

Table 2
Results of the augmented Lagrangian method for the bilateral contact and Tresca friction laws in comparison with the number of degrees of freedom (dof), the number of contact nodes (nbc), the Newton iterations (Nit) and the total CPU time (CPU) in seconds.

nbc	8	16	32	64	128	256	512
dof	92	198	650	2580	10280	41040	164000
Nit	5	9	9	11	10	11	9
CPU	<1	<1	<1	5	23	145	807

Now, we can compare the efficiency of the implemented algorithms.

Performances of the algorithms. In Table 1, we provide the number of degrees of freedom (dof), the number of Newton iterations (Nit) for the convergence of the Active set method for the bilateral contact associated with Tresca friction laws and the total CPU time required to reach the convergence (CPU) in second for several values of the number of contact nodes on the boundary Γ_3 (nbc), i.e. several discretizations. We conduct the same study for the Augmented Lagrangian method (Table 2).

At first and even though it becomes only clear when $nbc > 64$, if we were to consider only the number of iterations, it seems the Augmented Lagrangian method is slightly more efficient than the Active set method. However, in the same time, it also appears that the latter is much faster CPU time-wise than the former, almost twice as fast. Such a behavior was to be expected; we can assume it arises from the fact that the active set method do not require to use Lagrange multipliers. It implies that the linear system arising from the nonlinear problem is smaller for the active set method, as confirmed by the comparison between the number of *dof* in both cases, and may be less ill conditioned than the original augmented system, a well-known characteristic of frictional contact problems.

8.2. Unilateral contact and Coulomb friction example

For $nbc = 128$ depicted in Fig. 6, 9728 2D elastic elements were considered for 10024 dof. The behavior of the interaction between the foundation and the deformable body is depicted by a unilateral constraint combined with a Coulomb's law of friction.

We provide below the value of the parameters used for the computation:

$E = 100\ \mathrm{N/m^2}, \quad \kappa = 0.3,$
$\boldsymbol{f}_0 = (0,0)\ \mathrm{N/m^2}, \quad \boldsymbol{f}_2 = (0,-0.1)\,\mathrm{N/m} \quad \text{on } \Gamma_2,$
$c_v = 10, \quad c_\tau = 10, \quad r_{lagrangian} = 0.1, \quad \mu = 0.2,$
stopping criterion : $\epsilon = 10^{-6}$

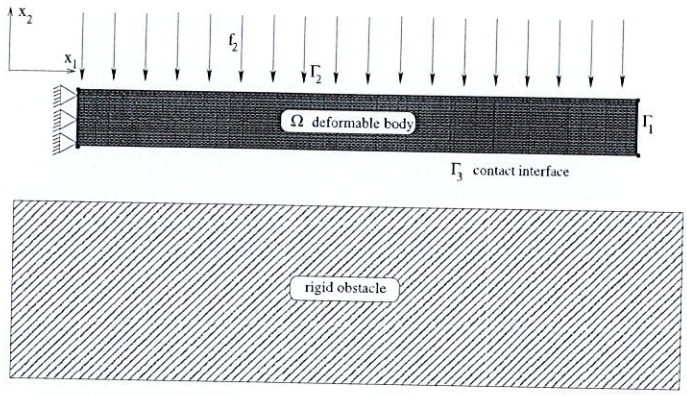

Fig. 6. Physical setting of the unilateral beam against a foundation.

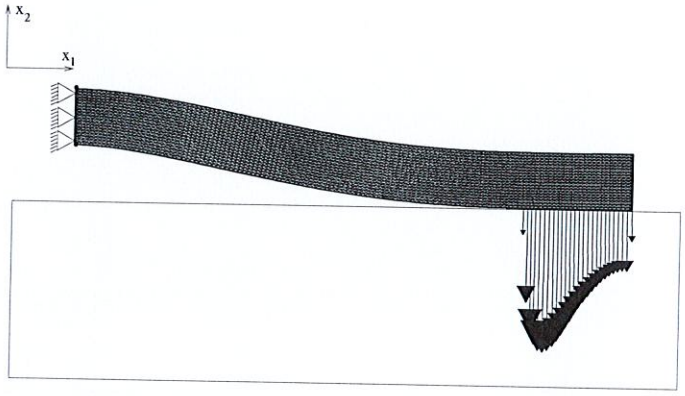

Fig. 7. Deformed configuration of the unilateral beam against a foundation.

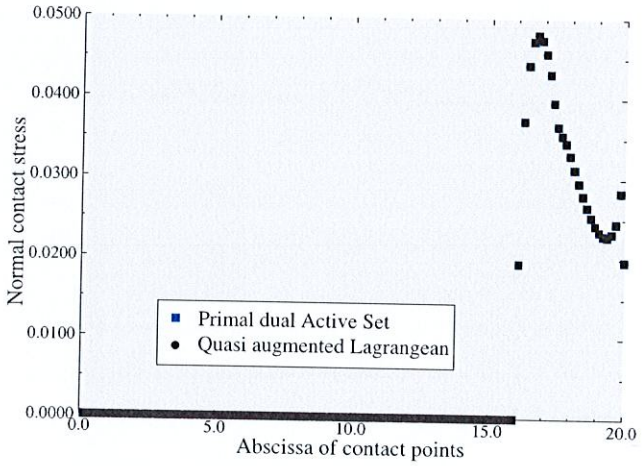

Fig. 8. Normal contact stresses on the contact area.

In Fig. 7, we plot the normal contact stresses and the deformed configuration on the boundary Γ_3.

Accuracy of the active set method comparing to the augmented Lagrangian method.

Once again, we assess the accuracy of the active set method by comparing it to the well-known Augmented Lagrangian. The boundary Γ_3 is divided into 128 equal parts; the normal contact stress σ_ν and tangential friction stress $\|\sigma_\tau\|$ with respect to the abscissa are plotted in Figs. 4 and 5 for each method. Once again, it turns out that for the contact stress computed by both methods, be it σ_ν or $\|\sigma_\tau\|$, there is no visible difference ($\approx 1.10^{-7}$), thus confirming the accuracy on this test case (see Figs. 8 and 9).

Performances of the algorithms. In Table 3, we provide the number of degrees of freedom (dof), the number of Newton iterations (Nit) for the convergence of the Active set method regarding the unilateral contact combined with Tresca friction

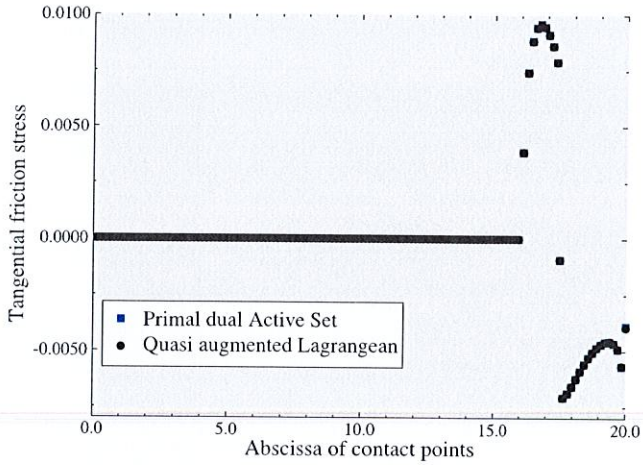

Fig. 9. Tangential friction stresses on the contact area.

Table 3
Results of the active set method for the unilateral contact and Coulomb friction laws in comparison with the number of degrees of freedom (dof), the number of contact nodes (nbc), the Newton iterations (Nit), the fixed point iterations (fpit) and the total CPU time (CPU) in seconds.

nbc	8	16	32	64	128	256	512
dof	76	166	586	2414	10024	40528	162976
Nit	15	25	37	45	44	46	39
fpit	5	5	5	5	5	5	7
CPU	<1	<1	1	9	61	364	1448

Table 4
Results of the augmented Lagrangian method for the unilateral contact and Coulomb friction laws in comparison with the number of degrees of freedom (dof), the number of contact nodes (nbc), the Newton iterations (Nit) and the total CPU time (CPU) in seconds.

nbc	8	16	32	64	128	256	512
dof	92	198	650	2580	10280	41040	164000
Nit	4	17	20	23	26	27	28
CPU	<1	<1	1	9	62	405	2972

law, the number of fixed point iterations (fpit) to approximate the Coulomb friction law and the total CPU time (CPU) in second for several values of the number of contact nodes on the boundary Γ_3 (nbc), i.e. several discretizations. We conduct the same study for the Augmented Lagrangian method for the unilateral contact and Coulomb friction laws (Table 4). In this case, unlike the previous configuration, the number of Newton iteration is no longer appropriate to compare both methods, as the active set method approximates the Coulomb friction with an extra inner loop involving a succession of states of Tresca friction while the Augmented Lagrangian method does not. Therefore, the only reliable criterion available is the CPU time. Despite this extra loop, out of the two methods, the active set method remains the fastest. Given the result obtained in the last case, for $nbc = 512$, we can even infer the gap between the two methods widen as the number of degrees of freedom increases. Such an assumption should be confirmed for more complex problems.

9. Numerical simulations in the dynamic case

As we assess the performances and accuracy of the active set methods implemented on simple static cases, our aim is now to evaluate the robustness of these methods on more complex problems. We carried out these simulations based on two dynamic contact configurations: the unilateral contact with a Coulomb's law of friction of a linear elastic beam and the bounce of a hyper-elastic ring, both on a perfectly rigid foundation. Once again, the numerical solution of Problem $\mathcal{P}$ is computed with both the active set method and the augmented Lagrangian method in order to highlight the performances of the former compared to the latter. As for the first numerical examples, the domain Ω depict the cross section of a three-dimensional deformable body subjected to the action of initial velocity so that a plane stress hypothesis can be assumed. Note that, as we already validated the accuracy of the active set methods, since a dynamic configuration does not inherently significantly change the active set procedure and to keep the article at reasonable length, we consider there is no need to linger any longer about accuracy.

9.1. Academic example: compression of a beam against a perfectly rigid foundation

The reference configuration is the same as the one introduced in Section 8.2.

Table 5
Results of the active set method for the unilateral contact and Coulomb friction laws in comparison with the number of degrees of freedom (dof), the number of contact nodes (nbc), the total numbers of Newton iterations (Ntit), the average fixed point iterations (afpit) and the total CPU time (CPU) in seconds.

nbc	8	16	32	64	128	256	512
dof	76	166	586	2414	10024	40528	162976
Ntit	119	153	191	254	258	240	216
afpit	4	4	4	4	5	4	5
CPU	0.07	0.33	2.52	25.57	162.28	861.92	3295.57

Table 6
Results of the augmented Lagrangian method for the unilateral contact and Coulomb friction laws in comparison with the number of degrees of freedom (dof), the number of contact nodes (nbc), the total numbers of Newton iterations (Ntit) and the total CPU time (CPU) in seconds.

nbc	8	16	32	64	128	256	512
dof	92	198	650	2580	10280	41040	164000
Ntit	37	58	80	87	98	112	119
CPU	0.04	0.28	2.25	20.05	113.78	769.38	5773.57

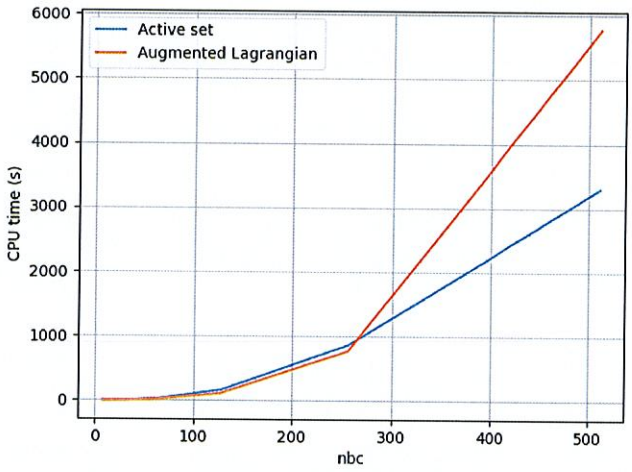

Fig. 10. Active set and augmented lagrangian CPU time with respect to *nbc*.

We provide below the value of the parameters used for the computation (see Tables 5–8).

$\rho = 1000\ \text{kg/m}^3, \quad T = 0.5\ \text{s}, \quad k = \frac{1}{10},$
$E = 10\ \text{N/m}^2, \quad \kappa = 0.3,$
$\boldsymbol{f}_0 = (0, 0)\ \text{N/m}^2, \quad \boldsymbol{f}_2 = (0, -0.1)\,\text{N/m} \quad \text{on } \Gamma_2,$
$c_v = 10, \quad c_\tau = 10, \quad r_{lagrangian} = 0.1, \quad \mu = 0.2$
stopping criterion : $\epsilon = 10^{-6}$.

In this specific case, it appears that the active set method only performs better than the Augmented Lagrangian method for $nbc > 512$ (see Tables 5–6). However, as shown in Fig. 10, we can safely assume that the more nodes in contact we have, the more the gap in CPU time between the methods will widen, making the active set method all the more relevant.

9.2. Relevant example: Bounce of a hyper-elastic ring against a perfectly rigid foundation

We now introduce another representative configuration to assess the performances of the active set type methods in a large deformation framework. It is a relevant example of friction contact problem, namely a hyper-elastic ring bouncing on a perfectly rigid foundation.

Let *nbc* be the number of nodes on Γ. Here, as depicted in Fig. 11, the boundary Γ_3 is divided into 128 equal parts, 1664 hyper-elastic 2D elements were used for 2048 dof. The compressible material response, is described by a variant of the Ogden constitutive law (cf [41]) defined by this energy density function

$$W(\mathbf{C}) = c_1(I_1 - 3) + c_2(I_2 - 3) + a(I_3 - 1) - (c_1 + 2c_2 + a)\ln I_3.$$

With I_1, I_2 and I_3, the three invariants of the tensor $\mathbf{C}$, with $\mathbf{C} = \mathbf{F}^T\mathbf{F}$.

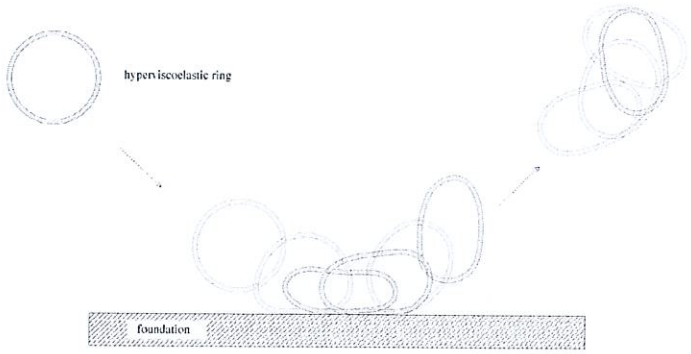

Fig. 11. Sequence of the deformed hyper-elastic ring before, during and after impact.

Table 7
Results of the active set method for the unilateral contact and Coulomb friction laws in comparison with the number of degrees of freedom (dof), the number of contact nodes (nbc), the total numbers of Newton iterations (Ntit), the average fixed point iterations (afpit) and the total CPU time (CPU) in seconds.

nbc	32	64	128	256	512
dof	192	384	1792	4608	15 360
Ntit	1876	1904	1944	1961	2022
afpit	4	4	4	4	4
CPU	6.32	12.39	99.22	304.62	1841.23

Table 8
Results of the augmented Lagrangian method for the unilateral contact and Coulomb friction laws in comparison with the number of degrees of freedom (dof), the number of contact nodes (nbc), the total numbers of Newton iterations (Ntit) and the total CPU time (CPU) in seconds.

nbc	32	64	128	256	512
dof	256	512	2048	5120	16 384
Ntit	1462	1568	1705	1782	1866
CPU	8.59	18.03	139.69	428.80	2693.86

Next, we provide below a description of the physical setting.

$$\Omega = \left\{(x_1, x_2) \in \mathbb{R}^2 : \ 81 < (x_1 - 100)^2 + (x_2 - 100)^2 < 100\right\},$$
$$\Gamma_1 = \varnothing, \qquad \Gamma_2 = \varnothing,$$
$$\Gamma_3 = \left\{(x_1, x_2) \in \mathbb{R}^2 : \ (x_1 - 100)^2 + (x_2 - 100)^2 = 100\right\}.$$

The ring is thrown toward a foundation given by $\left\{(x_1, x_2) \in \mathbb{R}^2 : \ x_2 \leq -50\right\}$, as shown in Fig. 11, with an initial velocity at 45° angle. For the discretization, we use 1664 elastic nodes and 128 contact nodes. For the numerical experiments, the data are:

$$\rho = 1000 \text{ kg/m}^3, \quad T = 5 \text{ s}, \quad k = \tfrac{1}{500},$$
$$\boldsymbol{u}_0 = (0, 0) \text{ m}, \quad \boldsymbol{u}_1 = (10, -10) \text{ m/s},$$
$$c_1 = 0.5 \text{ MPa}, \quad c_2 = 0.05 \text{ MPa}, \quad a = 0.5 \times 10^{-4} \text{ MPa},$$
$$c_v = 10, \quad c_\tau = 10, \quad r_{lagrangian} = 0.1$$
$$g = 50 \text{ m}, \quad \mu = 0.2,$$
$$\text{stopping criterion} : \epsilon = 10^{-6}.$$

As in the previous section, we compare the results obtained by the active set type method and the augmented Lagrangian method (see Tables 7–8).

Even though it is the most complex case considered so far, the performances do not decrease. As shown in Fig. 12, once again it seems that the more number of nodes in contact we have, the more the gap in CPU time between the methods will widen, which is consistent with our assumption in the previous. However, this is not enough to explain the gain in CPU time for the Inexact Active Set method comparing to the Quasi Lagrangian method. As mentioned at the end of Section 7, for the former, the linearized systems are symmetrical, even in a frictional case, while the increased linearized ones are not, for the latter.

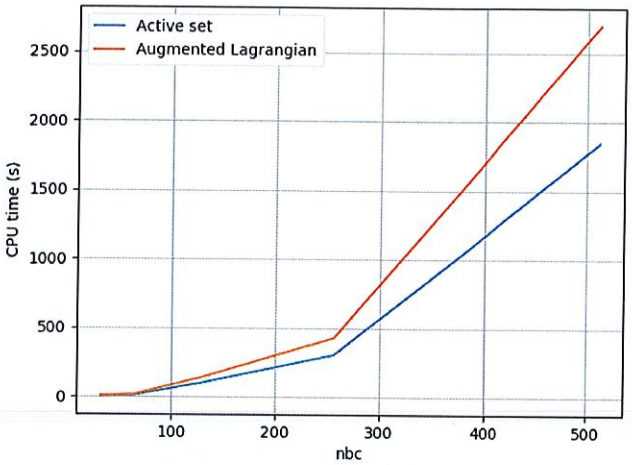

Fig. 12. Active set and augmented lagrangian CPU time with respect to *nbc*.

It clearly shows the robustness of the active set method in a complex configuration. It seems that avoiding the Lagrange multipliers is still a relevant and strong argument in favor of the Active set type methods, comparing to the classical Augmented Lagrangian method.

10. Conclusion

A concise analysis of several active set methods through classical problems arising in Contact Mechanics, for instance unilateral/bilateral contact associated with Tresca's/Coulomb's law of friction, has been presented in this work. Indeed, we established a variational formulation from the hyper-elastodynamic problem along with a numerical approximation of the problem and we provided a minimization formulation through the augmented Lagrangian formalism. From there on, we proposed an overview of various active set type methods, recalling the one introduced in [26] in the frictionless case and extending it to the bilateral contact case with Tresca's law of friction, then to the unilateral case with Coulomb's law of friction with their algorithms. We also considered an alternative for the latter based on the approximation of the Coulomb's law by a succession of states of Tresca friction in which the friction threshold is fixed at each fixed point iteration (cf [21]). Introducing such a combination, and highlighting its relevance on a hyper-elastodynamic problem, is one of the main contribution of this work. In order to assess the behavior of the active set type methods, we performed numerical simulations. We carried them out on four test cases, two in static and two in dynamic, with the augmented Lagrangian method taken as reference: three in the small deformation framework by considering a beam and one in the large deformation framework with the bounce of a hyper-elastic ring against a rigid foundation.

As a first result, and despite the fact that it is not a reliable criterion in the Coulomb's case, it turns out that the active set methods take more iterations than the Augmented Lagrangian to converge. However, they also seem to be faster in terms of CPU time than the augmented Lagrangian. This can be explained by the fact that the linear system arising from the nonlinear problem is smaller for the active set methods, symmetric even in a 2D frictional case, and that it might be better conditioned. Nevertheless, and as it was mentioned before, the fact that the active set type methods do not require the use of the Lagrange multipliers cannot be neglected from an implementation point of view. Therefore, for all these reasons, it seems consistent to consider an active set type method over the augmented Lagrangian method, even in a friction case.

At this point, we can already highlight some prospects which could be considered in the continuation of this paper. From an analytical point of view, a challenging prospect would be to prove the convergence of the inexact primal–dual active set with fixed point method, which remains for now an open question, at the best of our knowledge. Moreover, the method has been developed as a nodal method, i.e. the status of each zone is determined using the values at the nodes of the mesh. A generalization to an integral formulation will be investigated in the future. From a numerical point of view, it would be interesting to study whether such a method could be extended even further to multibody contact problems, for instance those arising in granular mechanics.

We would like to thank the Reviewers for the attention paid to this article and in particular for their comments and corrections.

Acknowledgments

The project has received funding from the European Union's Horizon 2020 Research and Innovation Programme under the Marie Sk lodowska-Curie grant agreement No. 823731 – CONMECH.

References

[1] P. Alart, A. Curnier, A mixed formulation for frictional contact problems prone to Newton like solution methods, Comput. Methods Appl. Mech. Engrg. 92 (1991) 353–375.
[2] F. Ben Belgacem, P. Hild, P. Laborde, Extension of the mortar finite element method to a variational inequality modeling unilateral contact, Math. Models Methods Appl. Sci. 9 (1999) 287–303.
[3] F. Ben Belgacem, Y. Renard, Hybrid finite element methods for the signorini problem, Math. Comp. 72 (243) (2003) 1117–1145.
[4] P. Chabrand, F. Dubois, M. Raous, Various numerical methods for solving unilateral contact problems with friction, Math. Comput. Modelling 28 (4–8) (1998) 97–108.
[5] F. Chouly, M. Fabre, P. Hild, R. Mlika, J. Pousin, Y. Renard, An overview of recent results on nitsche's method for contact problems, Lect. Notes Comput. Sci. Eng. 121 (2017) 93–141.
[6] W. Han, M. Sofonea, Quasistatic Contact Problems in Viscoelasticity and Viscoplasticity, in: Studies in Advanced Mathematics, vol. 30, American Mathematical Society–International Press, 2002.
[7] H. Khenous, P. Laborde, Y. Renard, Mass redistribution method for finite element contact problems in elastodynamics, Eur. J. Mech. A Solids 27 (5) (2008) 918–932.
[8] F. Lebon, Contact problems with friction: models and simulations, Simul. Model. Pract. Theory 11 (5–6) (2003) 449–463.
[9] T. Laursen, Computational Contact and Impact Mechanics, Springer, Berlin, 2002.
[10] M. Raous, P. Chabrand, F. Lebon, Numerical methods for solving unilateral contact problem with friction, numéro spécial, J. Méc. Théor. Appl. 7 (1988) 111–128.
[11] M. Sofonea, A. Matei, Mathematical Models in Contact Mechanics, in: London Mathematical Society Lecture Note Series, vol. 398, Cambridge University Press, Cambridge, 2012.
[12] P. Wriggers, Computational Contact Mechanics, Wiley, Chichester, 2002.
[13] N. Kikuchi, J.T. Oden, Contact Problems in Elasticity: A Study of Variational Inequalities and Finite Element Methods, in: SIAM Studies in Applied Mathematics, vol. 8, Philadelphia, 1988.
[14] J.T. Oden, S.J. Kim, Interior penalty methods for finite element approximations of the signorini problem in elastostatics, Comput. Math. Appl. 8 (1) (1982) 35–56.
[15] G. De Saxcé, Z.-Q. Feng, New inequality and functional for contact with friction: the implicit standard material approach, Mech. Struct. Mach. 19 (1991) 301–325.
[16] S. Dumont, On enhanced descend algorithms for solving frictional multi-contact problems : applications to the discrete element method, Internat. J. Numer. Methods Engrg. 93 (2013) 1170–1190.
[17] P. Joli, Z.-Q. Feng, Uzawa and newton algorithms to solve frictional contact problems within the bi-potential framework, Internat. J. Numer. Methods Engrg. 73 (3) (2008) 317–330.
[18] F. Chouly, An adaptation of nitsche's method to the tresca friction problem, J. Math. Anal. Appl. 411 (2014) 329–339.
[19] F. Chouly, P. Hild, Y. Renard, A nitsche finite element method for dynamic contact : 1. Semi-discrete problem analysis and time-marching schemes, ESAIM: M2AN 49 (2) (2015) 481–502.
[20] M. Hintermuller, K. Ito, K. Kunish, The primal dual active set strategy as a semismooth Newton method, SIAM J. Optim. 13 (2002) 865–888.
[21] S. Hueber, G. Stadler, B.I. Wohlmuth, A primal dual active set algorithm for three-dimensional contact problems with coulomb friction, SIAM J. Sci. Comput. 30 (2) (2008) 572–596.
[22] S. Hueber, B.I. Wohlmuth, A primal dual active set strategy for non-linear multibody contact problems, Comput. Methods Appl. Mech. Engrg. 194 (27–29) (2005) 3147–3166.
[23] M. Hintermuller, V. Kovtunenko, K. Kunish, Semismooth Newton methods for a class of unilaterally constrained variational problems, Adv. Math. Sci. Appl. 147 (2004) 513–535.
[24] G. Duvaut, J.L. Lions, Les inÉquations En Mécanique et en Physique, Dunod, 1972.
[25] C. Licht, E. Pratt, M. Raous, Remarks on a numerical method for unilateral contact including friction, Unilateral Probl. Struct. Anal. (1991) 129–144.
[26] S. Abide, M. Barboteu, D, Danan analysis of two active set type methods for unilateral contact problems, Appl. Math. Comput. 284 (2016) 286–307.
[27] P.G. Ciarlet, Mathematical Elasticity, I : Three-Dimensional Elasticity, in: Series Studies in Mathematics and its Applications, North-Holland, Amsterdam, 1988.
[28] P. Le Tallec, Numerical methods for nonlinear three-dimensional elasticity, in: P.G. Ciarlet, J.L. Lions (Eds.), Handbook of Numerical Analysis, Vol. III, North-Holland, 1994.
[29] K. Poulios, Y. Renard, An unconstrained integral approximation of large sliding frictional contact between deformable solids, Comput. Struct. 153 (2015) 75–90.
[30] J.J. Moreau, in: Zorski (Ed.), Application of Convex Analysis to Some Problems of Dry Friction, in: Trends of Pure Mathematics Applied to Mechanics, 1979.
[31] M. Barboteu, L. Gasinski, P. Kalita, Analysis of a dynamic frictional contact problem for hyperviscoelastic material with non-convex energy density, Math. Mech. Solids 23 (3) (2018) 359–391.
[32] Y. Ayyad, M. Barboteu, Formulation and analysis of two energy-consistent methods for nonlinear elastodynamic frictional contact problems, J. Comput. Appl. Math. 228 (2009) 254–269.
[33] Y. Ayyad, M. Barboteu, J.R. Fernández, A frictionless viscoelastodynamic contact problem with energy-consistent properties: Numerical analysis and computational aspects, Comput. Methods Appl. Mech. Engrg. 198 (5–8) (2009) 669–679, 15.
[34] M. Barboteu, K. Bartosz, P. Kalita, An analytical and numerical approach to a bilateral contact problem with nonmonotone friction, Int. J. Appl. Math. Comput. Sci. 23 (2013) 263–276.
[35] M. Barboteu, K. Bartosz, P. Kalita, A dynamic viscoelastic contact problem with normal compliance, finite penetration and nonmonotone slip rate dependent friction, Nonlinear Anal. Real. 22 (2015) 452–472.
[36] M. Barboteu, K. Bartosz, P. Kalita, A. Ramadan, Analysis of a contact problem with normal compliance, finite penetration and nonmonotone slip dependent friction, Comm. Cont. Math. 16 (2014) 1350016.
[37] H.B. Khenous, P. Laborde, Y. Renard, On the discretization of contact problems in elastodynamics, Lect. Notes Appl. Comput. Mech. 27 (2006) 31–38.
[38] H.B. Khenous, J. Pommier, Y. Renard, Hybrid discretization of the signorini problem with Coulomb friction, theoretical aspects and comparison of some numerical solvers, Appl. Numer. Math. 56 (2006) 163–192.
[39] M. Barboteu, D. Danan, M. Sofonea, in: W. Han, et al. (Eds.), A Hyper-Elastic Dynamic Frictional Contact Model with Energy-Consistent Properties, in: Advances in Mechanics and Mathematics, vol. 33, Springer International Publishing, Switzerland, 2015, http://dx.doi.org/10.1007/978-3-319-14490-010.
[40] G. Pietrzak, A. Curnier, Large deformation frictional contact mechanics: continuum formulation and augmented Lagrangian treatment, Comput. Methods Appl. Mech. Engrg. 177 (4) (1999) 351–381.
[41] P.G. Ciarlet, G. Geymonat, Sur les lois de comportement en élasticité non-linéaire compressible, C. R. Acad. Sci. 295 (I) (1982) 423–426.